37. Cologne JB, Tokuoka S, Beebe GW, et al. Effects of radiation on incidence of primary liver cancer among atomic bomb survivors. *Radiat Res* 1999; 153:364–73.
38. Walsh L. A short review of model selection techniques for radiation epidemiology. *Radiat Environ Biophys* 2007;46:205–13.
39. Sieghart W, Pinter M, Hucke F, et al. A single determination of C-reactive protein at the time of diagnosis predicts long term outcome of patients with hepatocellular carcinoma. *Hepatology* 2013; 57:2224–34.
40. Zimmermann E, Anty R, Tordjman J, et al. C-reactive protein levels in relation to various features of non-alcoholic fatty liver disease among obese patients. *J Hepatol* 2011;55: 660–5.
41. Yoneda M, Mawatari H, Fujita K, et al. High-sensitivity C-reactive protein is an independent clinical feature of nonalcoholic steatohepatitis (NASH) and also of the severity of fibrosis in NASH. *J Gastroenterol* 2007;42: 573–82.
42. Wands J. Hepatocellular carcinoma and sex. *N Engl J Med* 2007;357:1974–6.
43. Sander LE, Trautwein C, Liedtke C. Is interleukin-6 a gender-specific risk factor for liver cancer? *Hepatology* 2007;46:1304–5.
44. Prieto J. Inflammation, HCC and sex: IL-6 in the centre of the triangle. *J Hepatol* 2008;48:380–1.
45. Porta C, De Amici M, Quaglini S, et al. Circulating interleukin-6 as a tumor marker for hepatocellular carcinoma. *Ann Oncol* 2008;19:353–8.
46. Grivennikov S, Karin M. Autocrine IL-6 signaling: a key event in tumorigenesis? *Cancer Cell* 2008;13:7–9.
47. Pradhan AD, Manson JE, Rifai N, et al. C-reactive protein, interleukin 6, and risk of developing type 2 diabetes mellitus. *JAMA* 2001;286:327–34.
48. Cologne J, Langholz B. Selecting controls for assessing interaction in nested case-control studies. *J Epidemiol* 2003;13:193–202.

RADIATION RESEARCH 180, 60–69 (2013)
0033-7587/13 $15.00

DOI: 10.1667/RR3183.1

Effects of *IL-10* Haplotype and Atomic Bomb Radiation Exposure on Gastric Cancer Risk

Tomonori Hayashi,[a,1] Reiko Ito,[a] John Cologne,[b] Mayumi Maki,[a] Yukari Morishita,[a] Hiroko Nagamura,[a] Keiko Sasaki,[a] Ikue Hayashi,[c] Kazue Imai,[a] Kengo Yoshida,[a] Junko Kajimura,[a] Seishi Kyoizumi,[a] Yoichiro Kusunoki,[a] Waka Ohishi,[d] Saeko Fujiwara,[d] Masazumi Akahoshi[e] and Kei Nakachi[a]

[a] *Department of Radiobiology/Molecular Epidemiology, Radiation Effects Research Foundation, Hiroshima, Japan;* [b] *Department of Statistics, Radiation Effects Research Foundation, Hiroshima, Japan;* [c] *Central Research Laboratory, Hiroshima University Faculty of Dentistry, Hiroshima, Japan;* [d] *Clinical Studies, Radiation Effects Research Foundation, Hiroshima, Japan; and* [e] *Department of Clinical Studies, Radiation Effects Research Foundation, Nagasaki, Japan*

Hayashi, T., Ito, R., Cologne, J., Maki, M., Morishita, M., Nagamura, H., Sasaki, K., Hayashi, I., Imai, K., Yoshida, K., Kajimura, J., Kyoizumi, S., Kusunoki, Y., Ohishi, W., Fujiwara, S., Akahoshi, M. and Nakachi, K. Effects of *IL-10* Haplotype and Atomic Bomb Radiation Exposure on Gastric Cancer Risk. *Radiat. Res.* 180, 60–69 (2013).

Gastric cancer (GC) is one of the cancers that reveal increased risk of mortality and incidence in atomic bomb survivors. The incidence of gastric cancer in the Life Span Study cohort of the Radiation Effects Research Foundation (RERF) increased with radiation dose (gender-averaged excess relative risk per Gy = 0.28) and remains high more than 65 years after exposure. To assess a possible role of gene-environment interaction, we examined the dose response for gastric cancer incidence based on immunosuppression-related *IL-10* genotype, in a cohort study with 200 cancer cases (93 intestinal, 96 diffuse and 11 other types) among 4,690 atomic bomb survivors participating in an immunological substudy. Using a single haplotype block composed of four haplotype-tagging SNPs (comprising the major haplotype allele *IL-10-ATTA* and the minor haplotype allele *IL-10-GGCG*, which are categorized by *IL-10* polymorphisms at −819A>G and −592T>G, +1177T>C and +1589A>G), multiplicative and additive models for joint effects of radiation and this *IL-10* haplotyping were examined. The *IL-10* minor haplotype allele(s) was a risk factor for intestinal type gastric cancer but not for diffuse type gastric cancer. Radiation was not associated with intestinal type gastric cancer. In diffuse type gastric cancer, the haplotype-specific excess relative risk (ERR) for radiation was statistically significant only in the major homozygote category of *IL-10* (ERR = 0.46/Gy, $P = 0.037$), whereas estimated ERR for radiation with the minor *IL-10* homozygotes was close to 0 and nonsignificant. Thus, the minor *IL-10* haplotype might act to reduce the radiation related risk of diffuse-type gastric cancer. The results suggest that this *IL-10* haplotyping might be involved in development of radiation-associated gastric cancer of the diffuse type, and that *IL-10* haplotypes may explain individual differences in the radiation-related risk of gastric cancer.

[1]Address for correspondence: Department of Radiobiology/Molecular Epidemiology, Radiation Effects Research Foundation, 5-2 Hijiyama Park, Minami-ku, Hiroshima 732-0815, Japan. e-mail: tomo@rerf.or.jp.

INTRODUCTION

Even now, more than 60 years after the atomic bombings, rates of certain cancers in atomic bomb survivors are significantly elevated in a dose-dependent manner (*1–4*). Widely accepted mechanisms of radiation carcinogenesis include direct damage to cellular oncogenes and tumor suppressor genes, and other late effects by which mutations of these genes occur in later years (e.g., bystander effects; genomic instability), eventually leading to malignant transformation of directly-exposed, surrounding and offspring cells. No definite conclusion has been reached concerning whether the immune system is involved in these mechanisms. In the study of late effects of atomic bomb radiation, it is important to elucidate gene-radiation interaction—the impact of past radiation exposure may work differently on cancer risks of individuals who have different genetic backgrounds, particularly related to immune and inflammatory responses.

Some reports suggest that functional polymorphisms in genes regulating the immune and inflammatory response may contribute to susceptibility to, and clinical outcome with, gastric cancer (GC) (*5–7*). Interleukin-10 (IL-10) is an important immunoregulatory cytokine mainly produced by activated T cells, monocytes, B cells and thymocytes. It has important anti-inflammatory and immunosuppressive activities, including the ability to downregulate T helper 1 (Th1) cytokine and macrophage costimulatory molecule expression (*8*). IL-10 has been shown to inhibit various immune functions, such as antigen presentation, cytokine production, macrophage activation and antigen-specific T-cell proliferation (*9, 10*). By interfering with antigen-presenting cells, IL-10 reduces antigen-specific T-cell proliferation. It has been postulated that IL-10 plays a key role in the

oncogenic and metastatic ability of neoplasms (*11, 12*). However, a large body of evidence in different animal tumor models shows that IL-10 can favor immune-mediated cancer rejection (*13–17*). The *IL-10* gene comprises five exons and is located on chromosome 1q31-32 (*18*). The promoter region contains at least 40 polymorphic sites according to dbSNP (http://www.ncbi.nlm.nih.gov/sites/snp). Three polymorphic promoter variants of IL-10, located at positions −1082 (A>G), −819 (T>C) and −592 (A>C), are associated with IL-10 production (*19, 20*) and gastric cancer risk (*21, 22*). It has also been reported that *IL-10 −819 TT* genotype is protective against gastric cancer relative to the *CC* and *TC* genotypes in Asians (*23*) and that the IL-10 −1082 G allele is associated with an increased risk of cardiac gastric cancer in Asians (*24*).

Several studies have demonstrated a possible involvement of IL-10 in the pathogenesis of gastric cancer (*22, 25–28*). A nested case–control study previously carried out within the Adult Health Study (AHS) cohort of atomic bomb survivors at the Radiation Effects Research Foundation, using stored sera and blood cells (*29, 30*), reported that radiation increases the risk of noncardia gastric cancer of diffuse type but not intestinal type (*31*). The aim of the present study was to examine the relationship between risk of intestinal- or diffuse-type gastric cancer and radiation dose based on inflammation-related *IL-10* gene polymorphisms among atomic bomb survivors. The effects of *IL-10* genotype and radiation exposure on plasma IL-10 levels were also examined.

MATERIALS AND METHODS

Study Population

The Radiation Effects Research Foundation (RERF) conducted a cohort study within the AHS of approximately 20,000 atomic bomb survivors. The AHS is a clinical research program based on biennial health examinations established in July, 1957 as the clinical subcohort of the Life Span Study (LSS) cohort of atomic bomb survivors in Hiroshima and Nagasaki, Japan. AHS subjects were selected from the LSS cohort stratified according to distance from the hypocenter at the time of bombing and presence or absence of acute symptoms. Subjects for a broad immunology study including the genome study were selected from the AHS subjects because blood samples are not available from other members of the LSS. The clinical data collected during these examinations facilitate long-term follow-up studies of disease incidence and changes in physiological and biochemical endpoints, which benefit participants and contribute to health management of the atomic bomb survivors. Between 1981–2002, we obtained blood samples from 7,131 AHS participants who visited the clinic for examinations as part of the broader immunology study. After excluding subjects who had a history of first primary cancer at the time of blood collection, whose radiation dose could not be estimated, who were exposed *in utero* (organ doses not estimable), who were aged 80 or older at the time of blood collection or who refused to provide informed consent (84 subjects), 4,690 subjects remained for analysis [3,175 subjects provided informed consent (1,515 subjects who were deceased after blood collection were approved for this study by the RERF Ethical Committee)]: we call this the "cancer and immuno-genome (IMG) cohort". As a part of the LSS study, incident cancer cases were detected by the Hiroshima Tumor and Tissue Registries and the Nagasaki Cancer Registries, which also provided data on histological classification. Histological classification of gastric cancer was based on the Japanese Research Society for gastric cancer classification until 1986, and subsequently on the WHO coding system (ICD-O, ICD-O-2 and ICD-O-3), which was converted into Lauren's classification as reported elsewhere (*32, 33*). Baseline for follow-up was defined as the date of the first blood sample for the IMG study (collection began in 1981). The end of follow-up was December 31, 2001, the latest date of complete cancer ascertainment as of the time the data analysis was initiated. Follow-up of individual subjects ended on the date of first primary cancer onset, date of death, or the end of cohort follow-up, whichever occurred first. During the follow-up period (maximum 21 years), 200 gastric cancer cases (93 intestinal, 96 diffuse and 11 other types) were identified.

Baseline characteristics of cases and cohort subjects are shown in Table 1. We analyzed linkage disequilibrium (LD) with 300 controls, performed association analysis between *IL-10* haplotypes and plasma IL-10 levels in 644 noncancer cohort members, and conducted risk estimation for radiation and *IL-10* haplotyping using 200 cases amidst the 4,690 IMG cohort subjects.

Ethical Consideration

This study was approved by the Ethical Committee (Human Investigation Committee) and by the Ethics Committee for Genome Research at the RERF.

Measurement of Plasma IL-10 Levels

We measured plasma IL-10 levels in the IMG cohort members using a highly sensitive enzyme-linked immunosorbent assay kit (Quantikine HS, R&D systems, Minneapolis, MN). The minimum detectable dose of IL-10 was 0.5 pg/mL. Six hundred forty-four subjects who did not have a cancer history were randomly selected from the IMG cohort members to exclude an effect of cancer history on the relationship between *IL-10* haplotype and plasma IL-10 levels.

Identification and Genotyping of SNPs

The Celera Genomic database including Asian populations (*34, 35*) was used to screen haplotype-tagging (ht) SNPs in the *IL-10* gene region, along with the detection of novel SNPs over the region using the NCBI database. We selected the 19 htSNPs with allele frequency >5% among Japanese. After examining allele frequency in the study population, we found that ten of the 19 htSNPs showed variant allele frequencies >5% in our study population. We therefore selected these ten htSNPs: *IL-10* −92952C>T (IL10-1, rs1400986), −64871T>C (IL10-2, rs2073186), −32510A>G (IL10-3, rs4347211), −23055T>C (IL10-4, rs11583394), −14378T>C (IL10-5, rs880790), −1082T>C (IL10-6, rs1800896), −819G>A (IL10-7, rs1800871), −592T>G (IL10-8, rs1800872), +1177T>C (IL10-9, rs1518111), and +1589A>G (IL10-10, rs1554286). To reduce time and labor, 300 noncancer cohort members from the nonexposed group in the IMG cohort were analyzed to identify *IL-10* haplotypes for these 10 htSNPs. Primers and probes for these htSNPs were designed using Primer Express software, version 2.1 (Applied Biosystems, Foster City, CA). The TaqMan-Allelic Discrimination method was used for the detection of SNPs. All of the assays were conducted in 384-well PCR plates. The principle of TaqMan Real-Time PCR assay system using fluorogenic probes and the 5′ nuclease is described by Livak (*36*). Amplification reactions (5 μl) were carried out in duplicate with 10 ng of template DNA, 1× TaqMan Universal Master Mix buffer (Applied Biosystems), 300 n*M* of each primer and 200 n*M* of each fluorogenic probe. Thermal cycling was initiated with 2 min incubation at 50°C, followed by a first denaturation step of 10 min at 95°C, and then by 40 cycles of 15 s at 95°C and of 1 min at 60°C. After PCR was completed, the plates were brought to room temperature and read in an ABI PRISM 7900 Sequence Detection

TABLE 1
Characteristics of the Study Subjects within the RERF Immuno-Genome Cohort and Others

	Cases		Cohort		Subjects other than IMG cohort	
Total[a]	200 (100)		4,690 (100)		15,476 (100)	
Age at the time of bombings[b]	21 (1–43)		18 (0–43)		33 (0–79)	
Age at entry[c]	59 (38–80)		56 (37–80)			
Gender[a]						
Men	111 (55.5)		1,642 (35.0)		6,328 (40.9)	
Women	89 (44.5)		3,048 (65.0)		9,148 (59.1)	
City[a]	Men	Women	Men	Women	Men	Women
Hiroshima	77 (69.4)	65 (73.0)	1,013 (61.7)	2,064 (67.7)	4,362 (68.9)	6,731 (73.6)
Nagasaki	34 (30.6)	24 (27.0)	629 (38.3)	984 (32.3)	1,966 (31.1)	2,417 (26.4)
Radiation dose[a]	Men	Women	Men	Women	Men	Women
<5 mGy	53 (47.7)	28 (31.5)	710 (43.2)	1,246 (40.9)	3,736 (59.0)	5,328 (58.2)
5–728[d]	27 (24.3)	32 (36.0)	423 (25.8)	943 (30.9)	1,250 (19.8)	2,121 (23.2)
≥728	31 (27.9)	29 (32.6)	509 (31.0)	859 (28.2)	1,342 (21.2)	1,699 (18.6)
Smoking status[a]	Men	Women	Men	Women		
Nonsmoking	41 (36.9)	64 (71.9)	728 (44.3)	2,672 (87.7)		
Quit smoking	9 (8.1)	3 (3.4)	233 (14.2)	110 (3.6)		
Smoking	46 (41.4)	8 (9.0)	636 (38.7)	190 (6.2)		
Unknown	15 (13.5)	14 (15.7)	45 (2.7)	76 (2.5)		
Histological type[e]						
Intestinal type	93 (46.5)					
Diffuse type	96 (48.0)					
Other types	11 (5.5)					
IL-10 haplotype						
Major homozygote	71 (35.5)		2,048 (43.8)			
Heterozygote	93 (46.5)		1,988 (42.5)			
Minor homozygote	33 (16.5)		492 (10.5)			
Others[a,f]	3 (1.5)		145 (3.1)			

[a]Number (%).
[b]Median (range).
[c]Median (5–95% percentiles).
[d]728 mGy: median dose in exposed cohort members.
[e]Gastric cancer cases are classified by intestinal, diffuse and other types (the intestinal type included tubular and papillary carcinomas, the diffuse type included adenocarcinomas, mucinous adenocarcinomas, and signet-ring adenocarcinomas, and the other types were five cases with cancer in adenoma, one with squamous or adenosquamous carcinoma and five not otherwise specified cases). These histological types are counted individually.
[f]Seventeen of 4,690 subcohort subjects could not be determined one or two genotypes in the *IL-10* haplotype.

System (Applied Biosystems). Results were analyzed using the Allelic Discrimination software (SNPAlyze, Dynacom, Yokohama, Japan).

Haplotype and Radiation Risk Analysis

Rate ratios or excess rate ratios for gastric cancer incidence were estimated using general risk models extending the standard proportional hazards time-to-event analysis for cohort follow-up data, with attained age as the underlying time axis and left truncation on age at the time of blood collection (*37, 38*). Analyses were performed using the Cox regression module (Peanuts) of Epicure (version 1.81, Hirosoft Inc., Seattle, WA). All statistical models were stratified on gender and included adjustment for year of birth, city (Hiroshima or Nagasaki) and smoking intensity (cigarettes per day). City was included in the background in all analyses to adjust for any potential confounders, since *IL-10* haplotype-specific risk for radiation may possibly differ by city due to potential involvement of other gene polymorphisms that are mechanistically associated with *IL-10* functions and differ by city. Information on smoking was obtained by interview at the time of blood collection. *IL-10* haplotypes were determined as described below. Atomic bomb radiation dose in weighted Gray (wGy) was estimated using the DS02 dosimetry system (*39*), based on weighted skin dose computed as the gamma dose plus 10 times the neutron dose. A radiation dose <0.005 Gy was called nonexposed when performing analyses based on dose group.

Regression analysis of gastric cancer incidence was based on histological subtype – intestinal or diffuse. Cases in this study were primary gastric cancers, which included 17 synchronous multiple cancer cases that experienced primary cancer(s) of other organs within one year before or after gastric cancer diagnosis. Censoring was imposed at the time of other primary cancer diagnosis, death or the end of cancer follow-up (December 31, 2001). An excess relative risk (ERR: excess rate ratio) model was used for radiation risk estimation with adjustment for gender using stratification and adjustment for smoking intensity and year of birth using a log-linear model.

For *IL-10* haplotypes, indicator variables for the three categories (major homozygote, heterozygote and minor homozygote) were used to estimate either the rate ratio (RR, in the case of multiplicative models using the standard log-linear Cox model for *IL-10* haplotypes) or ERR (in the case of additive models for the joint effect of haplotyping and radiation), with the major homozygotes treated as the reference category. In this study, we considered only heterozygotes involving the most frequent (major) and second-most frequent (minor) alleles among the numerous heterozygotes that appeared in the process

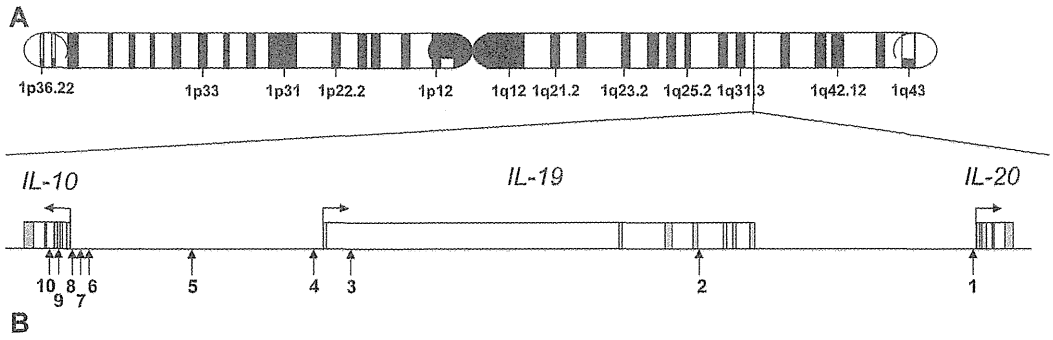

	IL10-1	IL10-2	IL10-3	IL10-4	IL10-5	IL10-6	IL10-7	IL10-8	IL10-9
IL10-1									
IL10-2	0.23								
IL10-3	0.01	0.00							
IL10-4	0.04	0.00	0.67						
IL10-5	0.03	0.00	0.58	0.85					
IL10-6	0.00	0.01	0.01	0.01	0.02				
IL10-7	0.04	0.01	0.05	0.09	0.10	0.09			
IL10-8	0.04	0.01	0.05	0.09	0.10	0.09	1.00		
IL10-9	0.04	0.01	0.05	0.09	0.10	0.09	1.00	1.00	
IL10-10	0.03	0.01	0.05	0.09	0.11	0.09	0.99	0.99	0.99

FIG. 1. Identification of haplotype block. Panel A: 10 SNPs examined in the 95 kb region spanning the *IL-10*, *IL-19* and *IL-20* loci (arrows with numbers from 1 to 10). Panel B: LD analysis of the *IL-10* htSNPs. The r^2 values between the ten htSNPs are shown, indicating strong LD among IL10-7, −8, −9 and −10.

of LD analysis. Four genomic models for *IL-10* haplotype effects were considered: arbitrary (no structure among the three *IL-10* haplotypes; the "categorical" genomic model); "linear" (a codominant model where the effect in heterozygotes is assumed to be one-half of the effect in minor homozygotes); "dominant" (the presence of one or two minor haplotype alleles confers the same risk); and "recessive" (risk occurs only in minor homozygotes). Statistical interaction (effect estimate modification) between radiation and *IL-10* haplotypes was tested on both multiplicative and additive scales (*40*). The multiplicative joint risk model is $r(g,d) = e^{\delta g}[1 + \beta d]$ and the additive joint risk model is $r(g,d) = 1 + \phi g + \gamma d$, with g being the haplotype (a two- or three-level factor) and d the radiation dose (a continuous variable). Both models specify a rate ratio $r(g,d)$ that multiplies the background incidence (incidence among nonexposed persons).

RESULTS

Identification of Haplotype Blocks

The ten htSNPs (IL-10-1 to −10) are located on one gene region spanning about 95 kb in length (Fig. 1A). When we examined all combinations between the ten htSNPs for LD, four of ten htSNPs formed one haplotype block with r^2 values greater than 0.9 (Fig. 1B) and generated two major haplotype alleles, wild allele *IL-10 -ATTA* and variant one *IL-10 -GGCG* (IL-10-7, −8, −9 and −10). These two haplotype alleles constituted 98.1% of all haplotype alleles available in this block, 65.9% for wild *IL-10 -ATTA* and 32.2% for variant *IL-10 -GGCG*. Posterior probabilities for these two haplotype alleles exceeded 0.99, so these haplotypes were treated as known.

IL-10 Haplotypes and Plasma IL-10 Levels

As these htSNPs are located in untranslated regions including the promoter regions, we examined the relationship between *IL-10* haplotypes and plasma IL-10 levels in 664 cancer-free IMG cohort members. Mean plasma IL-10 protein levels were 2.79 pg/ml (SD 1.85, CV 0.68) among persons with the major homozygote *IL-10* haplotype, 3.02 pg/ml (SD 2.36, CV 0.78) among heterozygotes and 3.69 pg/ml (SD 2.97, CV 0.81) among minor homozygotes. Using log transformed IL-10 protein levels, regression analysis revealed no difference in IL-10 protein levels between major homozygotes and heterozygotes ($P = 0.39$), but minor homozygotes had significantly higher levels ($P = 0.030$). Using a linear model for *IL-10* haplotype, there was a significant trend in number of minor haplotyope alleles ($P = 0.034$). Radiation dose was related to log plasma IL-10 protein levels with a relative change in actual protein levels (not log transformed) of $e^{0.1278} = 1.14$ (14% increase) at 1 Gy ($P < 0.001$). These results suggest that plasma IL-10 levels varied not only by genetic factors but also by radiation exposure, and might therefore be closely associated with gastric cancer risk.

TABLE 2
Relative Risk of Intestinal Type Gastric Cancer for Radiation and *IL-10* Haplotypes using a Multiplicative Model

Model	Haplotype RR (95% CI, *P* value) (log-linear model, adjusted for radiation)				
P value is for heterogeneity test with categorical haplotype or for comparison with categorical haplotype	Major homozygote (*AA*)	Heterozygote (*Aa*)	Minor homozygote (*aa*)	Radiation ERR (95% CI, *P* value) (adjusted for haplotypes)	Interaction *P* value
Numbers of cases	31	41	20		
Categorical haplotype ($P = 0.071$) (*aa*) or (*Aa*) vs. *AA*[ref] AIC[b] = 910.022	1 (referent)	1.38 (0.83 – 2.33, 0.21)	**2.22 (1.10 – 4.25, 0.027)**	−0.05 (−0.19 – 0.23, >0.5)	NA[a]
Linear ($P > 0.5$) *aa*(1) > *Aa*(½) > *AA*[ref] AIC = 908.106	1 (referent)	exp {log(RR[*aa*]) × ½} = 1.47	**2.16 (1.11 – 4.17, 0.024)**	−0.05 (−0.19 – 0.23, >0.5)	>0.5
Dominant ($P = 0.17$) (*aa*,*Aa*) vs. *AA*[ref] AIC = 909.950	1 (referent)	1.55 (0.96 – 2.53, 0.071)		−0.05 (−0.19 – 0.23, >0.5)	0.32
Recessive ($P = 0.20$) *aa* vs. (*Aa*,*AA*)[ref] AIC = 909.646	1 (referent)		1.87 (0.98 – 3.30, 0.057)	−0.06 (−0.19 – 0.21, >0.5)	0.30

[a]NA, could not be estimated.
[b]Akaike's information criteria.

The incidence rate ratio of all gastric cancer combined for women compared with men was 0.41 [95% confidence interval (CI) 0.28, 0.58; $P < 0.001$]. Incidence increased with smoking intensity (RR = 1.24 among smokers of 10 cigarettes/day compared with nonsmokers; 95% CI 1.07, 1.43; $P < 0.001$) and year of birth (rate increased with more recent years of birth; $P < 0.001$). With those adjustments, crude RRs for *IL-10* haplotypes were: 1.26 (*ATTA/GGCG* heterozygote; 95% CI 0.91, 1.75; $P = 0.17$) and 1.59 (minor homozygote; 95% CI 0.98, 2.50; $P = 0.062$), with heterogeneity test $P = 0.13$. The linear genomic model was statistically significant: risk for the minor homozygote was 1.60 (95% CI 1.03, 2.48; $P = 0.038$), with the risk for the *ATTA/GGCG* heterozygote being one-half of the risk for minor homozygote on the log scale (i.e., RR = exp{[ln(1.60)]/2} = 1.26). The other two types of one-parameter genomic models (dominant and recessive) did not produce significant effects ($P = 0.066$ with the dominant model, $P = 0.13$ with the recessive model).

There was no evidence of interaction between gender and *IL-10* haplotypes ($P = 0.23$). Crude (adjusted only for gender, smoking and birth year, but not for *IL-10* haplotypes) ERR of all gastric cancers for radiation was 0.11 (95% CI −0.05, 0.34; $P = 0.22$) and after adjustment for *IL-10* haplotypes using the categorical genomic model the ERR for radiation was 0.12 (95% CI −0.05, 0.36; $P = 0.19$). The main effect of *IL-10* haplotypes after adjustment for radiation was essentially the same as the crude risk with each genomic model. The best fitting genomic model, and only statistically significant parameter, was with the linear genomic model. However, the apparent effects of radiation and *IL-10* haplotypes with all gastric cancers combined reflect large differences in their effects according to subtypes (see below), hence results for interaction between these two factors with all gastric cancers combined are not reported.

Results for Intestinal Type Gastric Cancer

Crude proportions of cohort members with intestinal type gastric cancer increased with number of variant (*GGCG*) haplotype allele: 1.5% among those with the major (*ATTA*) *IL-10* homozygote, 2.0% with the *ATTA/GGCG* heterozygote, and 3.9% with the minor homozygote. Incidence was about twice as high in Hiroshima as in Nagasaki (RR for Nagasaki 0.41; 95% CI 0.22, 0.71; $P = 0.001$) and was significantly related to smoking intensity (RR for smoking 10 cigarettes/day 1.38; 95% CI 1.12, 1.66; $P = 0.004$).

The cohort distribution of haplotypes (major homozygote, *ATTA/GGCG* heterozygote, minor homozygote) was similar in the two cities: (0.45, 0.44, 0.11) in Hiroshima and (0.46, 0.43, 0.11) in Nagasaki. Given no apparent association between city and *IL-10* haplotypes, the city difference would not be expected to confound the *IL-10* risk, and indeed there was no noticeable difference in *IL-10* risk parameters depending on whether or not city was included in the background model. There was no evidence of an effect of radiation: after adjustment of background incidence for gender, birth year, city and smoking (not adjusting for *IL-10* haplotypes), radiation ERR/Gy was −0.06 (95% CI −0.19, 0.21; $P > 0.5$).

Tables 2 and 3 show the jointly estimated risks for radiation and *IL-10* haplotypes with intestinal type gastric cancer. Main effects for radiation and haplotypes were similar with either the multiplicative or the additive model, so ERRs for radiation and haplotypes in the additive model

TABLE 3
Excess Relative Risk of intestinal Type Gastric Cancer for Radiation by *IL-10* Haplotypes using an Additive Model

Model[b]	Radiation ERR with interaction (95% CI, *P* value) (radiation ERR specific to haplotypes)			
P value is for heterogeneity test with categorical haplotype or comparison with categorical haplotype (crude risk)	Major homozygote (*AA*)	Heterozygote (*Aa*)	Minor homozygote (*aa*)	Interaction *P* value
Numbers of cases	31	41	20	
Categorical haplotype ($P = 0.071$) (*aa*) or (*Aa*) vs. *AA*[ref] AIC[b] = 910.022	−0.13 (NA – 0.20, 0.30)	0.25 (−0.21, 1.00, >0.5)	−0.58 (NA[a] – NA, 0.25)	0.23
Codominant ($P > 0.5$) *aa*(1) > *Aa*(½)>*AA*[ref] AIC = 908.337	−0.11 (NA – 0.28, 0.42)	—	0.14 (NA – NA, NA)	>0.5
Dominant ($P = 0.17$) (*aa*,*Aa*) vs. *AA*[ref] AIC = 909.950	−0.13 (−0.21 – 0.20, 0.30)	0.09 (−0.33 – 0.72, >0.5)		0.39
Recessive ($P = 0.20$) *aa* vs. (*Aa*,*AA*)[ref] AIC = 909.646	−0.02 (NA – NA, NA)		−0.53 (NA– NA, NA)	0.29

[a]NA, could not be estimated.
[b]Akaike's information criteria.

are not shown. With intestinal type gastric cancer, there was evidence of a significant effect of *IL-10* haplotypes after adjustment for radiation (Table 2). As with all gastric cancers combined, the fit of the categorical genomic model was similar to that of the linear genomic model, but the RRs were larger than with all gastric cancers combined. The linear genomic model had the lowest value of Akaike information criterion (AIC), and the categorical model produced risk estimates for the minor homozygote and the *ATTA/GGCG* heterozygote that were consistent with those from the linear model (compare $\exp\{\ln[2.16]/2\} = 1.47$ from the linear model with 1.55 for major heterozygotes).

Although the intestinal subtype evidenced no overall effect of radiation, it is possible that radiation effects might exist if there were biologically significant interaction between radiation and *IL-10* haplotypes. It was not possible to estimate or test interaction between radiation and particular *IL-10* haplotypes with the categorical genomic model, but none of the estimable radiation ERRs with interaction in the multiplicative model were very far from 0 (not shown) and none of the interaction tests for the one-parameter genomic models produced significant results (Table 2). With the additive model, again there were no statistically significant interactions (Table 3) and there was no evidence of trend in radiation ERRs with frequency of minor haplotype allele (radiation ERR was higher with the *ATTA/GGCG* heterozygote relative to the major homozygote but lower with the minor homozygote; Table 3).

Results for Diffuse Type Gastric Cancer

Crude proportions of cohort members with diffuse type gastric cancer evidenced no association with *IL-10* haplotypes: 1.9% with the major (*ATTA*) homozygote, 2.3% with the *ATTA/GGCG* heterozygote and 2.0% with the minor (*GGCG*) homozygote. Incidence of diffuse type did not depend on city ($P = 0.49$) and there was no impact on rate ratios for *IL-10* haplotypes depending on whether or not city was included in the background model. Smoking was not significantly related to diffuse type gastric cancer: RR for smoking 10 cigarettes/day compared with nonsmokers was 1.15 (95% CI 0.91, 1.40; $P = 0.23$). However, smoking was left in the analyses to avoid potential confounding. The crude ERR for radiation (after adjustment for gender, birth year, city and smoking but not for *IL-10* haplotypes) was statistically significant (ERR/Gy = 0.33; 95% CI 0.03, 0.83; $P = 0.027$).

Tables 4 and 5 show the jointly estimated risks for radiation and haplotype for diffuse type gastric cancer. With diffuse type, there was no evidence of an effect of *IL-10* haplotypes after adjustment for radiation (Table 4). There was no significant evidence of interaction between radiation and *IL-10* on either the multiplicative (Table 4) or additive (Table 5) scale. However, the haplotype-specific ERR for radiation was statistically significant only in the major homozygote category of *IL-10* (Table 5), being higher than the overall ERR for radiation, whereas estimated ERR for radiation with the minor *IL-10* homozygote was close to 0 and nonsignificant. Thus, the minor *IL-10* haplotype might act to reduce radiation-related risk of diffuse type gastric cancer.

DISCUSSION

We investigated the association between gene polymorphisms in the anti-inflammatory cytokine *IL-10* gene region

TABLE 4
Relative Risk of Diffuse Type Gastric Cancer for Radiation and *IL-10* Haplotypes using a Multiplicative Model

Model	Haplotype RR (95% CI, *P* value) (log-linear model, adjusted for radiation)				
P value is for heterogeneity test with arbitrary haplotype or for comparison with arbitrary haplotype	Major homozygote (*AA*)	Heterozygote (*Aa*)	Minor homozygote (*aa*)	Radiation ERR (95% CI, *P* value) (adjusted for haplotypes)	Interaction *P* value
Numbers of cases	38	46	10		
Categorical haplotype ($P > 0.5$) (*aa*) or (*Aa*) vs. *AA*[ref] AIC[a] = 1,039.889	1 (referent)	1.15 (0.73 – 1.82) >0.5	0.87 (0.35 – 1.84, >0.5)	**0.33** **(0.03 – 0.83, 0.027)**	>0.5
Codominant ($P = 0.46$) *aa*(1) > *Aa*(½) > *AA*[ref] AIC = 1,038.444	1 (referent)	exp{log(RR[*aa*]) × ½} = 1.01	1.02 (0.52 – 1.94, >0.5)	**0.32** **(0.03 – 0.82, 0.029)**	>0.5
Dominant ($P > 0.5$) (*aa*,*Aa*) vs. *AA*[ref] AIC = 1,038.338	1 (referent)	1.09 (0.71 – 1.71, >0.5)		**0.33** **(0.03 – 0.82, 0.028)**	>0.5
Recessive ($P > 0.5$) *aa* vs. (*Aa*,*AA*)[ref] AIC = 1,038.153	1 (referent)	0.81 (0.34 – 1.64, >0.5)		**0.32** **(0.03 – 0.82, 0.029)**	>0.5

[a]Akaike's information criteria.

and gastric cancer risk using a cohort study setting. *IL-10* haplotypes were significantly related to the risk of intestinal type gastric cancer, but not to the diffuse type. On the other hand, radiation was significantly associated with an increased risk of diffuse type gastric cancer. Regarding statistical interaction between radiation and *IL-10*, there was a suggestion of a trend towards lower radiation risk of the diffuse type with an increased number of variant *IL-10* haplotype allele, and only the *IL-10* major homozygote evidenced a statistically significant risk elevation by radiation when the radiation ERR was separately estimated by *IL-10* haplotype category. In addition, plasma IL-10 levels among noncancer cohort members were associated with *IL-10* haplotypes and increased with radiation dose, demonstrating the functional significance of this *IL-10* haplotyping and implying a joint effect of genetic factors and radiation in IL-10 expression.

Although the linear model was the best-fitting genomic model, we cannot conclude based on statistical criteria that it is the correct model. Furthermore, four genomic models were tested, leading to the possibility of spurious findings due to multiple testing. A Bonferroni correction would result in reducing the significance level from 0.05–0.0125, but due to a high degree of correlation among the genomic models the Bonferroni correction is inappropriate and a multiple-testing correction taking the correlation into account would not result in much change of significance level. We are therefore confident that the effect of *IL-10* for intestinal type gastric cancer based on the linear genomic model ($P = 0.038$) is unlikely to be a spurious result.

Observational studies lack power for detecting statistical interactions (*40*), and biological interactions—usually defined as departure from additive effects (*41*)—can therefore go undetected. The advantages of our study are long-term follow-up, detailed dosimetry reconstruction, and a well-defined radiation-exposed population. A limitation is the small number of subjects, particularly cases of gastric cancer, due to the size of the original cohort and exclusion criteria. Thus, lack of statistical significance does not necessarily imply lack of meaningful biological interaction. With intestinal type gastric cancer, not only were the interaction tests not statistically significant, the haplotype-specific radiation ERR estimates did not suggest any consistent pattern, being higher among the major heterozygotes and lower among the minor homozygotes, compared with the major homozygote. Nevertheless, were such a pattern biologically significant, it could explain the absence of overall radiation effect for intestinal type gastric cancer because the haplotype-specific ERRs would tend to cancel in the overall (no interaction) radiation ERR estimate. With diffuse type gastric cancer, there was some evidence of lack of additivity for joint effects of *IL-10* and radiation, with radiation risk being high and statistically significant among the major homozygote but low and nonsignificant among the minor homozygote. The lack of statistically significant interaction test in the additive model could be due to lack of power. Indeed, there was no statistically significant interaction on either the additive or multiplicative scale, but one or the other must require a statistical interaction term depending on which is the more appropriate model representing the joint biological effects (*42*).

To increase statistical power we included synchronous gastric cancer cases diagnosed within one year of other, first-primary cancer diagnoses. Although some of these cases could have been diagnosed through greater surveillance resulting from prior cancer, we think that is unlikely in

TABLE 5
Excess Relative Risk of Diffuse Type Gastric Cancer for Radiation by *IL-10* Haplotypes using an Additive Model

Model [b]	Radiation ERR with interaction (95% CI, *P* value) (radiation ERR specific to haplotypes)			
P value is for heterogeneity test with arbitrary haplotype or comparison with arbitrary haplotype (crude risk)	Major homozygote (*AA*)	Heterozygote (*Aa*)	Minor homozygote (*aa*)	Interaction *P* value
Numbers of cases	38	46	10	
Categorical haplotype ($P > 0.5$) (*aa*) or (*Aa*) vs. *AA*[ref] AIC[b] = 1,039.889	**0.46** **(0.02 – 1.43, 0.037)**	0.29 (−0.25 – 1.14, 0.33)	0.12 (NA[a] – NA, >0.5)	>0.5
Codominant ($P = 0.46$) *aa*(1) > *Aa*(½)>*AA*[ref] AIC = 1,038.444	**0.45** **(0.02 – 1.33, 0.034)**	—	0.08 (NA – 1.08, >0.5)	>0.5
Dominant ($P > 0.5$) (*aa*,*Aa*) vs. *AA*[ref] AIC = 1,038.338	**0.46** **(0.02 – 1.43, 0.037)**	0.25 (−0.23 – 0.97, 0.33)		>0.5
Recessive ($P > 0.5$) *aa* vs. (*Aa*,*AA*)[ref] AIC = 1,038.153	**0.34** **(0.03 – 0.88, 0.027)**		0.10 (NA – NA, >0.5)	>0.5

[a]NA, could not be estimated.
[b]Akaike's information criteria.

the case of gastric cancer. It is also unlikely that such cases are due to treatment for prior cancer because of the induction and latency periods for cancer growth and detection. However, we repeated the analyses of Tables 2–5 using as cases only first primary gastric cancers, with multiple cancer diagnoses (other cancer diagnosed at the same time as gastric cancer) or nonfirst-primary gastric cancers (gastric cancer diagnosed within one year of prior first-primary cancer) treated as censored at the time of first cancer diagnosis (the same as was done with all other cancer diagnoses in the analysis). There was no significant impact on results, except for slightly lower precision as would be expected with fewer cases. For example, with diffuse type gastric cancer, numbers of first-primary cases were 36, 44 and 10 (versus 38, 46 and 10 in Tables 4 and 5). The radiation ERR among major homozygotes was the same (0.45) but with slightly wider confidence interval (0.02–1.36 vs. 0.02–1.33) and slightly higher *P* value (0.038 vs. 0.034).

It is difficult to directly compare our results with those of previous studies in the atomic bomb survivors (*31*) because the nested case-control study that examined subtypes of gastric cancer involves a separately selected sample of cases with different follow-up period and the Life Span Study incidence analyses do not include subtype. Subtype will be considered in future LSS analyses but results are not yet available.

The Gram-negative bacterium Helicobacter pylori (H. pylori) is a well established etiologic factor, which works to elicit a chronic inflammatory response in the gastric mucosa and closely relates to the development of intestinal type gastric cancer (*43*). Differing inflammatory responses among hosts may help to explain different outcomes for persons infected with H. pylori, and therefore, consideration of *H. pylori* infectious status as well as gene polymorphisms involved in the host response to this infection might help further estimation of the radiation risks for *H. pylori*-infected and noninfected populations. This will be considered in future studies.

Regulatory mechanisms of immune suppression and inflammatory cytokine production inhibition of IL-10 are not fully understood. However, immune suppression of IL-10 may play an important role in the development of gastric cancer. From these results, we assessed the possibility of measurement of surrogate biomarkers, such as plasma IL-10 levels, for real-time estimation of gastric cancer risk as a model for prevention of gastric cancer. This idea came to us because the findings suggested that plasma IL-10 level is affected by both genetic and environmental factors, such as radiation exposure, and is closely associated with gastric cancer risk. We hope that further details of the relationship between gastric cancer risk and biomarkers clarified by future studies will enable us to better estimate gastric cancer risk, contributing to innovative preventive measures in atomic bomb survivors as well as other populations exposed to high levels of radiation in general, on the basis of both genetic and radiation factors.

ACKNOWLEDGMENTS

The Radiation Effects Research Foundation (RERF), Hiroshima and Nagasaki, Japan is a private, nonprofit foundation funded by the Japanese Ministry of Health, Labour and Welfare (MHLW) and the U.S. Department of Energy (DOE), the latter in part through DOE Award DE-HS0000031 to the National Academy of Sciences. This publication

was supported by RERF Research Protocols RPs 1–93, 4-04, 5-04, and 3–09 and was supported in part by the Grant-in-Aid for Scientific Research (B) from the Ministry of Education, Culture, Sports, Science, and Technology of Japan (24390162), and the Grant-in-Aid for Cancer Research from the Ministry of Health and Welfare of Japan (22090501). The views of the authors do not necessarily reflect those of the two governments.

Received: September 4, 2012; accepted: March 5, 2013; published online: June 17, 2013

REFERENCES

1. Pierce DA, Preston DL. Radiation-related cancer risks at low doses among atomic bomb survivors. Radiat Res 2000; 154:178–86.
2. Pierce DA, Shimizu Y, Preston DL, Vaeth M, Mabuchi K. Studies of the mortality of atomic bomb survivors. Report 12, Part I. Cancer: 1950–1990. Radiat Res 1996; 146:1–27.
3. Shimizu Y, Kato H, Schull WJ. Studies of the mortality of A-bomb survivors. 9. Mortality, 1950–1985: Part 2. Cancer mortality based on the recently revised doses (DS86). Radiation research 1990; 121:120–41.
4. Shimizu Y, Kato H, Schull WJ. Risk of cancer among atomic bomb survivors. J Radiat Res (Tokyo) 1991; 32 Suppl 2:54–63.
5. Peek RM, Jr. Pathogenesis of Helicobacter pylori infection. Springer Semin Immunopathol 2005; 27:197–215.
6. Rosenstiel P, Hellmig S, Hampe J, Ott S, Till A, Fischbach W, et al. Influence of polymorphisms in the NOD1/CARD4 and NOD2/CARD15 genes on the clinical outcome of Helicobacter pylori infection. Cell Microbiol 2006; 8:1188–98.
7. Seno H, Satoh K, Tsuji S, Shiratsuchi T, Harada Y, Hamajima N, et al. Novel interleukin-4 and interleukin-1 receptor antagonist gene variations associated with non-cardia gastric cancer in Japan: comprehensive analysis of 207 polymorphisms of 11 cytokine genes. J Gastroenterol Hepatol 2007; 22:729–37.
8. Mocellin S, Marincola FM, Young HA. Interleukin-10 and the immune response against cancer: a counterpoint. J Leukoc Biol 2005; 78:1043–51.
9. Taga K, Mostowski H, Tosato G. Human interleukin-10 can directly inhibit T-cell growth. Blood 1993; 81:2964–71.
10. de Waal Malefyt R, Haanen J, Spits H, Roncarolo MG, te Velde A, Figdor C, et al. Interleukin 10 (IL-10) and viral IL-10 strongly reduce antigen-specific human T cell proliferation by diminishing the antigen-presenting capacity of monocytes via downregulation of class II major histocompatibility complex expression. J Exp Med 1991; 174:915–24.
11. Wojciechowska-Lacka A, Matecka-Nowak M, Adamiak E, Lacki JK, Cerkaska-Gluszak B. Serum levels of interleukin-10 and interleukin-6 in patients with lung cancer. Neoplasma 1996; 43:155–8.
12. Avradopoulos K, Mehta S, Blackinton D, Wanebo HJ. Interleukin-10 as a possible mediator of immunosuppressive effect in patients with squamous cell carcinoma of the head and neck. Ann Surg Oncol 1997; 4:184–90.
13. Kundu N, Beaty TL, Jackson MJ, Fulton AM. Antimetastatic and antitumor activities of interleukin 10 in a murine model of breast cancer. J Natl Cancer Inst 1996; 88:536–41.
14. Huang S, Ullrich SE, Bar-Eli M. Regulation of tumor growth and metastasis by interleukin-10: the melanoma experience. J Interferon Cytokine Res 1999; 19:697–703.
15. Adris S, Klein S, Jasnis M, Chuluyan E, Ledda M, Bravo A, et al. IL-10 expression by CT26 colon carcinoma cells inhibits their malignant phenotype and induces a T cell-mediated tumor rejection in the context of a systemic Th2 response. Gene therapy 1999; 6:1705–12.
16. Ding Y, Qin L, Kotenko SV, Pestka S, Bromberg JS. A single amino acid determines the immunostimulatory activity of interleukin 10. J Exp Med 2000; 191:213–24.
17. Sato T, Terai M, Tamura Y, Alexeev V, Mastrangelo MJ, Selvan SR. Interleukin 10 in the tumor microenvironment: a target for anticancer immunotherapy. Immunologic Res 2011; 51:170–82.
18. Eskdale J, Kube D, Tesch H, Gallagher G. Mapping of the human IL10 gene and further characterization of the 5′ flanking sequence. Immunogenetics 1997; 46:120–8.
19. Suarez A, Castro P, Alonso R, Mozo L, Gutierrez C. Interindividual variations in constitutive interleukin-10 messenger RNA and protein levels and their association with genetic polymorphisms. Transplantation 2003; 75:711–7.
20. Turner DM, Williams DM, Sankaran D, Lazarus M, Sinnott PJ, Hutchinson IV. An investigation of polymorphism in the interleukin-10 gene promoter. Eur. J. Immunogenet 1997; 24:1–8.
21. El-Omar EM, Rabkin CS, Gammon MD, Vaughan TL, Risch HA, Schoenberg JB, et al. Increased risk of noncardia gastric cancer associated with proinflammatory cytokine gene polymorphisms. Gastroenterology 2003; 124:1193–201.
22. Sugimoto M, Furuta T, Shirai N, Nakamura A, Kajimura M, Sugimura H, et al. Effects of interleukin-10 gene polymorphism on the development of gastric cancer and peptic ulcer in Japanese subjects. J Gastroenterol Hepatol 2007; 22:1443–9.
23. Xue H, Lin B, An J, Zhu Y, Huang G. Interleukin-10-819 promoter polymorphism in association with gastric cancer risk. BMC Cancer 2012;12: 102.
24. Zhou Y, Li N, Zhuang W, Liu GJ, Wu TX, Yao X, et al. Interleukin-10 −1082 promoter polymorphism associated with gastric cancer among Asians. Eur J Cancer 2008; 44:2648–54.
25. Lee JY, Kim HY, Kim KH, Kim SM, Jang MK, Park JY, et al. Association of polymorphism of IL-10 and TNF-A genes with gastric cancer in Korea. Cancer Lett 2005; 225:207–14.
26. Bai XL, Sun LP, Liu J, Chen W, Zhang Y, Yuan Y. [Correlation of interleukin-10-1082G/a single nucleotide polymorphism to the risk of gastric cancer in north China: a case-control study]. Ai Zheng 2008; 27:35–40.
27. Xiao H, Jiang Y, Li R, Xia B. [Association of IL-10 gene polymorphisms with gastroduodenal diseases in Hubei Han population]. Zhonghua Yi Xue Yi Chuan Xue Za Zhi 2009; 26:423–6.
28. Chen KF, Li B, Wei YG, Peng CJ. Interleukin-10 −819 promoter polymorphism associated with gastric cancer among Asians. J Int Med Res 2010; 38:1–8.
29. Yamada M, Wong FL, Fujiwara S, Akahoshi M, Suzuki G. Noncancer disease incidence in atomic bomb survivors, 1958–1998. Radiat research 2004; 161:622–32.
30. Wong FL, Yamada M, Sasaki H, Kodama K, Akiba S, Shimaoka K, et al. Noncancer disease incidence in the atomic bomb survivors: 1958–1986. Radiat Res 1993; 135:418–30.
31. Suzuki G, Cullings H, Fujiwara S, Hattori N, Matsuura S, Hakoda M, et al. Low-positive antibody titer against Helicobacter pylori cytotoxin-associated gene A (CagA) may predict future gastric cancer better than simple seropositivity against H. pylori CagA or against H. pylori. Cancer Epidemiol Biomarkers Prev 2007; 16:1224–8.
32. Hanai A, Fujimoto I. Cancer incidence in Japan in 1975 and changes of epidemiological features for cancer in Osaka. Natl Cancer Inst Monograph 1982; 62:3–7.
33. Kaneko S, Yoshimura T. Time trend analysis of gastric cancer incidence in Japan by histological types, 1975–1989. Br J Cancer 2001; 84:400–5.
34. De La Vega FM, Dailey D, Ziegle J, Williams J, Madden D, Gilbert DA. New generation pharmacogenomic tools: a SNP linkage disequilibrium Map, validated SNP assay resource, and high-throughput instrumentation system for large-scale genetic studies. Biotechniques 2002; Suppl: 48–50, 2,4.
35. Venter JC, Adams MD, Myers EW, Li PW, Mural RJ, Sutton GG,

et al. The sequence of the human genome. Science 2001; 291:1304–51.

36. Livak KJ. Allelic discrimination using fluorogenic probes and the 5′ nuclease assay. Biomol Eng 1999; 14:143–9.

37. Preston DL, Shimizu Y, Pierce DA, Suyama A, Mabuchi K. Studies on mortality of atomic bomb survivors: Solid cancer and noncancer disease mortality: 1950–1997. RERF Report No 24-02, Radiation Effects Research Foundation, Hiroshima, Japan.

38. Cologne J, Hsu WL, Abbott RD, Ohishi W, Grant EJ, Fujiwara S, et al. Proportional hazards regression in epidemiologic follow-up studies: an intuitive consideration of primary time scale. Epidemiology 2012; 23:565–73.

39. Cullings HM, Fujita S, Funamoto S, Grant EJ, Kerr GD, Preston DL. Dose estimation for atomic bomb survivor studies: its evolution and present status. Radiat Res 2006; 166:219–54.

40. Greenland S. Tests for interaction in epidemiologic studies: a review and a study of power. Stat Med 1983; 2:243–51.

41. Rothman KJ, Greenland S, Walker AM. Concepts of interaction. Am J Epidemiol 1980; 112:467–70.

42. Cologne JB, Pawel DJ, Sharp GB, Fujiwara S. Uncertainty in estimating probability of causation in a cross-sectional study: joint effects of radiation and hepatitis-C virus on chronic liver disease. J Radiol Protect 2004; 24:131–45.

43. de Vries AC, Haringsma J, Kuipers EJ. The detection, surveillance and treatment of premalignant gastric lesions related to Helicobacter pylori infection. Helicobacter 2007; 12:1–15.

Mutation Research 755 (2013) 49–54

Contents lists available at SciVerse ScienceDirect

Mutation Research/Genetic Toxicology and Environmental Mutagenesis

journal homepage: www.elsevier.com/locate/gentox
Community address: www.elsevier.com/locate/mutres

Radiation-dose response of *glycophorin A* somatic mutation in erythrocytes associated with gene polymorphisms of *p53 binding protein 1*

Kengo Yoshida[a,*], Yoichiro Kusunoki[a], John B. Cologne[b], Seishi Kyoizumi[a], Mayumi Maki[a], Kei Nakachi[a], Tomonori Hayashi[a]

[a] *Department of Radiobiology/Molecular Epidemiology, Radiation Effects Research Foundation, Hiroshima, Japan*
[b] *Department of Statistics, Radiation Effects Research Foundation, Hiroshima, Japan*

ARTICLE INFO

Article history:
Received 12 March 2013
Received in revised form 4 May 2013
Accepted 6 May 2013
Available online 13 May 2013

Keywords:
Gene polymorphism
Radiation
Somatic mutation

ABSTRACT

Information on individual variations in response to ionizing radiation is still quite limited. Previous studies of atomic-bomb survivors revealed that somatic mutations at the *glycophorin A* (*GPA*) gene locus in erythrocytes were significantly elevated with radiation exposure dose, and that the dose response was significantly higher in survivors with subsequent cancer development compared to those without cancer development. Noteworthy in these studies were great inter-individual differences in *GPA* mutant fraction even in persons with similar radiation doses. It is hypothesized that persistent *GPA* mutations in erythrocytes of atomic-bomb survivors are derived from those in long-lived hematopoietic stem cell (HSC) populations, and that individual genetic backgrounds, specifically related to DNA double-strand break repair, contribute to individual differences in HSC mutability following radiation exposure. Thus, we examined the relationship between radiation exposure, *GPA* mutant fraction in erythrocytes, and single nucleotide polymorphisms (SNPs) of the key gene involved in DNA double-strand break repair, *p53 binding protein 1* (*53BP1*). *53BP1* SNPs and inferred haplotypes demonstrated a significant interaction with radiation dose, suggesting that radiation-dose response of *GPA* somatic mutation is partly dependent on *53BP1* genotype. It is also possible that 53BP1 plays a significant role in DNA double-strand break repair in HSCs following radiation exposure.

1. Introduction

Ionizing radiation induces DNA single/double-strand breaks, which leads to various biological processes such as apoptosis and somatic mutations, but information on individual variations among biological phenotypes in response to radiation exposure is still limited [1]. Previous cohort studies of atomic-bomb survivors in Hiroshima and Nagasaki showed that *glycophorin A* mutant fraction (*GPA* Mf) in erythrocytes was significantly elevated with increased radiation dose, and that the dose response was significantly higher in survivors subsequently diagnosed with cancer than in cancer-free individuals, especially among those survivors who were exposed to high-dose radiation (>1.5 Gy) [2,3]. The *GPA* Mf observed in erythrocytes of atomic-bomb survivors was assumed to be derived from mutations in long-lived hematopoietic stem cell (HSC) populations [2]. Noteworthy in the previous studies were great inter-individual differences in somatic gene mutation even in persons with similar radiation exposure doses, and thus far no significant effects on the dose response of *GPA* Mf have been detected based on these factors: age at exposure, gender, city (Hiroshima or Nagasaki), and smoking. Considering the existence of heritable radiosensitivity syndromes such as ataxia telangiectasia, we assume that genetic factors are involved in individual differences in somatic mutability and radiation-dose response of *GPA* Mf.

Although the molecular mechanism of *GPA* mutation remains elusive due to difficulty in the DNA-level analysis, hemizygous *GPA* mutant variants are thought to arise from point mutation, deletion, or chromosome loss, whereas homozygous *GPA* variants presumably arise from mitotic recombination, chromosome loss and reduplication, or gene conversion [4]. Because radiation-dose responses of *GPA* Mf are evaluated based on the frequency of hemizygous variants, a majority of radiation-induced *GPA* variants in A-bomb survivors are considered to be deletion-type mutations, which are known to frequently result from non-homologous end joining (NHEJ) repair following DNA double-strand breaks (DSBs) induced by radiation. In this study, we thus anticipated that the

Abbreviations: *GPA* Mf, *glycophorin A* mutant fraction; HSC, hematopoietic stem cell; *53BP1*, *p53 binding protein 1*.

* Corresponding author at: Department of Radiobiology/Molecular Epidemiology, Radiation Effects Research Foundation, 5-2 Hijiyama Park, Minami Ward, Hiroshima 732-0815, Japan. Tel.: +81 82 261 3131; fax: +81 82 261 3170.
E-mail address: kyoshi@rerf.or.jp (K. Yoshida).

1383-5718/$ – see front matter © 2013 Elsevier B.V. All rights reserved.
http://dx.doi.org/10.1016/j.mrgentox.2013.05.003

capacity of host cells to repair DSBs is a factor in somatic mutation following radiation exposure, and that differences in this capacity are linked to polymorphisms of genes involved in the process of DSB repair. There are at least two molecular pathways that can sense and repair DSBs: NHEJ and homologous recombination-mediated repair [5]. NHEJ pathway plays a dominant role in the repair of radiation-induced DSBs during the G1 phase of the cell cycle, and a pivotal mediator of this pathway is p53 binding protein 1 (53BP1) [6,7]. Recent studies suggest that 53BP1 is a very early sensor of DSBs as well as an indispensable mediator in DSB repair at higher doses [8,9], and that it is involved in the etiology of human cancers [10]. In animal models, *53BP1*-deficient mice exhibit immune deficiency, high radiation sensitivity and tumor development—these are features of a defective DNA damage response [9,11]. Moreover, NHEJ cannot accurately reconstitute sequence information at DSBs, so it is likely to result in somatic mutations at the site of repair [12].

This study thus targeted *53BP1* genotype to seek a molecular basis for the individually-differing radiation-dose responses of somatic mutation in the human hematopoietic system by assessing the relationship between radiation exposure dose, *GPA* Mf and *53BP1* gene polymorphisms among 1500 atomic-bomb survivors.

2. Materials and methods

2.1. Study population

The Radiation Effects Research Foundation (RERF; formerly the Atomic Bomb Casualty Commission, ABCC), has conducted the Adult Health Study since 1958, when it enrolled 23,000 atomic bomb survivors in Hiroshima and Nagasaki for biennial health examinations in ABCC/RERF outpatient clinics. *GPA* Mf was measured from June 1988 to August 1996 using blood samples obtained from 1691 survivors participating in the Adult Health Study whose MN blood types had been found to be heterozygous by the hemagglutination test [3]. Between 1981 and 2002, these 1691 survivors donated separate blood samples from which DNA could be extracted. We excluded 165 survivors who had been diagnosed with cancer before *GPA* measurement because of potential effects of cancer development and therapy on *GPA* mutation, but we included 174 subjects who developed cancer after *GPA* measurement, for a total of 1526 subjects. Basic characteristics of study subjects are shown in Table 1. Radiation dose was weighted absorbed bone marrow dose (Gy), estimated as the γ-ray dose plus 10 times the neutron dose.

This study was approved by the Human Investigation Committee and the Ethics Committee for Genome Research at RERF.

2.2. GPA mutant fraction measurement

We had used data on Mϕ and Nϕ hemizygous type (a cell expresses a single allele) *GPA* Mf obtained from MN heterozygous donors in the previous study [3], so statistical analysis was undertaken using the mean of Mϕ and Nϕ hemizygous *GPA* Mf.

2.3. SNP genotyping

Three single nucleotide polymorphisms (SNPs) of *53BP1* previously reported to be associated with cancer risk and having minor allele frequency > 5% among Japanese were selected through Pub-Med searches along the NCBI dbSNP database [13–15]. The TaqMan-Allelic Discrimination method was used for genotyping SNPs [16]. Primers and probes for the 3 SNPs, as shown in Supplementary Table 1, were designed using Primer Express software (Applied Biosystems, Foster City, CA). PCR amplifications (5 μl) were carried out with 10 ng of template DNA, 1× TaqMan Universal Master Mix (Applied Biosystems), 300 nM of each primer and 200 nM of each fluorogenic probe in 384-well plates. Thermal cycling was initiated with a 2 min incubation at 50 °C, followed by a first denaturation step of 10 min at 95 °C, followed by 40 cycles of 15 s at 95 °C and of 1 min at 60 °C. After PCR amplification, the plates were read using an ABI PRISM 7900 Sequence Detection System (Applied Biosystems), and results were analyzed using the Allelic Discrimination software (Applied Biosystems).

2.4. Statistical analysis

Overall SNP frequencies were calculated, Hardy–Weinberg equilibrium (HWE) was tested, and haplotype posterior probabilities were estimated using PLINK (version 1.07, http://pngu.mgh.harvard.edu/purcell/plink/; [17]). HWE of the 3 SNPs was tested in PLINK using both exact and standard (asymptotic) tests. Effects of haplotype and radiation, as well as their interaction, on *GPA* Mf were analyzed with joint haplotyope estimation using the full statistical likelihood by the E–M algorithm using the `haplo.glm` procedure of the R `haplo.stats` software package. *GPA* Mf was handled as a continuous outcome using ordinary regression after taking the logarithm [2]. Percent of total variation in log *GPA* Mf explained by individual factors without adjustment for other factors (univariate R^2) was computed as one minus the ratio: residual mean squared error for a univariate (crude) regression model including the factor divided by that for the null model (with intercept only),

$$R^2_{\text{univariate}} = \frac{\text{RMSE}_{\text{null}} - \text{RMSE}_{\text{factor}}}{\text{RMSE}_{\text{null}}} = 1 - \frac{\text{RMSE}_{\text{factor}}}{\text{RMSE}_{\text{null}}},$$

where residual mean squared error was estimated as deviance divided by degrees of freedom (RMSE = deviance/df). In multivariate models, percent total variation explained (ΔR^2) was computed as the difference in R^2 values of the multivariate regression models with and without the factor of interest:

$$\Delta R^2_{\text{multivariate}} = \left[1 - \frac{\text{RMSE}_{\text{multivariate w/factor}}}{\text{RMSE}_{\text{null}}}\right] - \left[1 - \frac{\text{RMSE}_{\text{multivariate w/out factor}}}{\text{RMSE}_{\text{null}}}\right].$$

We also calculated a stratified $R^2_{\text{univariate}}$ for haplotype by subsetting the data into < 1.0 Gy and ≥ 1.0 Gy radiation dose. To test the primary hypothesis, *i.e.*, *53BP1* genotype impacts *GPA* Mf following radiation exposure, we performed ordinary regression analyses of log *GPA* Mf as an outcome variable, with radiation dose (bone marrow dose) and *53BP1* SNP/haplotype as explanatory variables, including a test for their interaction. Fits of one-parameter (dominant, co-dominant, and recessive) models were compared to assess the appropriate scale for genomic interaction. Statistical tests and confidence intervals are based on Wald statistics.

Occasionally one or more SNPs within a haplotype block was/were missing, probably due to low quality of DNA samples. Missing data can produce bias [18]—in fact, there was imbalance by city in terms of missing *53BP1* data (not shown)—and deleting subjects with partially informative data results in loss of power. The `haplo.glm` procedure estimates effects of haplotypes and their interaction with radiation using multiple imputation based on posterior haplotype probabilities. Because only major and minor haplotypes were considered (rare variants were all simply combined into an "other" category), and posterior probabilities for major and minor haplotypes were quite high (>97%) when one SNP at most was missing, we excluded nine subjects (1 with subsequent cancer) who had more than one missing SNP, thus limiting the analysis to 1507 subjects with no missing SNPs as well as 10 subjects with only one missing SNP.

3. Results

The total was 1526 subjects, 1352 non-cancer cases and 174 cancer cases, after excluding subjects who were diagnosed with cancer prior to *GPA* Mf measurement (Table 1). Table 2 shows the 3 SNPs of *53BP1* analyzed in this study and the minor allele frequencies according to cancer status. The distributions of these 3 SNP-based genotypes did not significantly depart from the Hardy-Weinberg equilibrium.

Factors significantly related to log *GPA* Mf in univariate analyses were: gender (R^2 = 0.9%; percent total variation in *GPA* Mf explained by gender), smoking (R^2 = 0.9%), and radiation (R^2 = 16%). After adjustment for gender, smoking, and radiation dose, the main effects of the three *53BP1* SNPs did not demonstrate any significant association with *GPA* Mf, but there was a significant interaction between the SNP (D353E)-based genotype and radiation dose (Table 3, p = 0.016, ΔR^2 = 0.3%). There was also a suggestive interaction between the SNP (K1136Q)-based genotype and radiation dose (p = 0.083, ΔR^2 = 0.1%). These results indicate that the radiation response of *GPA* Mf might be modulated by *53BP1* genotype.

Frequencies of the two primary haplotype alleles of *53BP1* estimated using the E–M algorithm are shown in Table 4. Numbers of missing SNP data are shown in Supplementary Table 2. Although the number of subjects with one or two missing loci of *53BP1* is small (12 subjects), excluding those subjects could result in bias if the missing-data mechanism is related to the effects being studied and the reduction in statistical power (as shown in Supplementary Table 3). Therefore, taking into account all possible haplotypes and each posterior probability, we conducted data analysis with multiple-imputation (N = 1517).

Table 5 shows the results of fitting co-dominant genomic model for *53BP1* haplotypes. The main effects of haplotype and radiation were based on a model with joint adjustment but no interaction. There was no relationship of *53BP1 GGC* haplotype allele with *GPA* Mf as the outcome (p = 0.93), but there was a significant

Table 1
Basic characteristic of subjects.

	Non-cancer cases	Cancer cases
Total	1352	174
Age at *GPA* measurement (yrs old)[a]	65.5 (10.0)	67.6 (9.3)
Gender[b]		
Men	441 (32.6)	84 (48.3)
Women	911 (67.4)	90 (51.7)
City[b]		
Hiroshima	890 (65.8)	109 (62.6)
Nagasaki	462 (34.2)	65 (37.4)
Smoking[c] (cigarettes per day)	0 (0–19)	0 (0–23.1)
Radiation dose[c] (Gy)	0.082 (0–1.810)	0.201 (0–2.438)
GPA Mf[c] ($\times 10^{-6}$)	20.5 (7.0–87.7)	23.8 (7.5–150.8)

[a] Mean (SD).
[b] Number (%).
[c] Median (5–95 percentiles).

Table 2
53BP1 SNPs analyzed along with the minor allele frequency.

SNP	NCBI dbSNP D	Minor allele	Frequency among all subjects ($N = 1526$)	Frequency among subjects without cancer ($N = 1352$)	Major allele
53BP1 −885	rs1869258	*G*	0.390	0.384	*T*
53BP1 D353E	rs560191	*G*	0.382	0.377	*C*
53BP1 K1136Q	rs2602141	*C*	0.393	0.378	*A*

Table 3
Association of individual *53BP1* SNPs with *GPA* Mf in univariate analyses and interaction between SNPs and radiation.

Factor	Log *GPA* Mf		
	Coefficient	*E*	*p*
53BP1 −885 (G)	0.008	0.027	0.76
53BP1 D353E (G)	−0.002	0.027	0.96
53BP1 K1136Q (C)	0.003	0.027	0.92
53BP1 −885 × radiation	−0.053	0.042	0.20
53BP1 D353E × radiation	−0.10	0.043	0.016
53BP1 K1136Q × radiation	−0.073	0.042	0.083

Results are from an ordinary regression model for log *GPA* Mf. Coefficients for the main effects of SNPs are adjusted for radiation in a model without the gene–radiation interaction term. The coefficient for each SNP represents the absolute difference in log *GPA* Mf, based on a co-dominant genomic model, comparing heterozygotes for each SNP to major homozygotes. Thus, the coefficient for minor homozygotes is twice the value of the coefficient for the heterozygotes. Adjustments were also made for gender and smoking intensity.

interaction with radiation dose: *GPA* Mf increased by a factor of $\exp\{0.466\} = 1.59$ for an increase of 1 Gy ($p < 0.001$), but with the interaction the increase with dose was by a factor of 1.69 among *TCA* major homozygotes and 1.53 among *GGC* minor homozygotes (interaction $p = 0.027$, $\Delta R^2 < 0.1\%$). Percent of total variation in *GPA* Mf explained by *53BP1* haplotype was only 0.11% among persons exposed to less than 1.0 Gy, but 1.64% among persons exposed to 1.0 Gy or more, which suggests that 53BP1 may have a significant effect on somatic mutation in the presence of radiation exposure causing DSBs. In addition, the same regression analyses as in Table 5 were conducted with Hiroshima and Nagasaki subjects separately (Supplementary Table 4). The results, although suggesting a more significant interaction in Nagasaki than in Hiroshima, were consistent with the calculations overall.

Because the test of interaction might have inflated the type-I (false positive) rate if the exposure part of the model was misspecified [19], a quadratic term in radiation dose was added (Table 6). The quadratic term was statistically significant (coefficient = −0.095, SE = 0.029, $p = 0.001$) leading to leveling off of the dose response of *GPA* Mf at high doses (see later plots). There was no significant interaction between *53BP1* haplotype and the quadratic radiation-dose parameter (not shown), but addition of the quadratic term to the radiation-dose response did not alter the interaction with the linear dose response term (coefficient = −0.093, SE = 0.043, $p = 0.031$). Similar results were obtained with both dominant and recessive genomic models (Supplementary Table 5). Figs. 1 and 2 are plots of the radiation-dose response of *GPA* Mf superimposed on untransformed data and grouped data, respectively, with the co-dominant genomic model for *53BP1* haplotypes, including interaction between *53BP1* haplotypes and the linear radiation-dose response term.

Table 4
Haplotype frequencies of *53BP1*.

53BP1 haplotype allele	Frequency
GCA	00099
GCC	0.0051
GGA	0.0017
GGC	0.3679
TCA	0.6058
TCC	0.0023
TGA	0.0028
TGC	0.0046

Haplotype frequencies are based on the E–M algorithm, and the two primary haplotypes are GGC and TCA.

Table 5
Association of *53BP1* haplotype with *GPA* Mf and interaction with radiation exposure dose.[a]

Factor	Log *GPA* Mf		
	Coefficient	SE	*p*
GGC hetero[b]	0.003	0.027	0.93
Radiation[c]	0.47	0.028	<0.001
GGC × radiation	−0.096	0.043	0.027

[a] Results are from an ordinary regression model for log *GPA* Mf. Coefficients for the main effects of haplotype and radiation are mutually adjusted in a model without the interaction term.
[b] The coefficient for haplotype represents the absolute difference in log *GPA* Mf, based on a co-dominant genomic model, comparing heterozygotes for that haplotype to major homozygotes. The coefficient for minor homozygotes is twice the value of the coefficient for heterozygotes.
[c] The coefficient for radiation represents the difference in log *GPA* Mf per Gy.

Table 6
Association of *53BP1* haplotype with *GPA* Mf and interaction with radiation exposure dose (linear-quadratic).

Factor	Log *GPA* Mf		
	Coefficient	SE	*p*
GGC hetero	0.002	0.027	0.94
Radiation (linear)	0.67	0.070	<0.001
(Quadratic)	−0.095	0.029	0.001
GGC × radiation	−0.093	0.043	0.031

Results are from an ordinary regression model for log *GPA* Mf. The coefficient for haplotype represents the absolute difference in log *GPA* Mf, based on a co-dominant genomic model. The coefficient for radiation represents the difference in log *GPA* Mf per Gy.

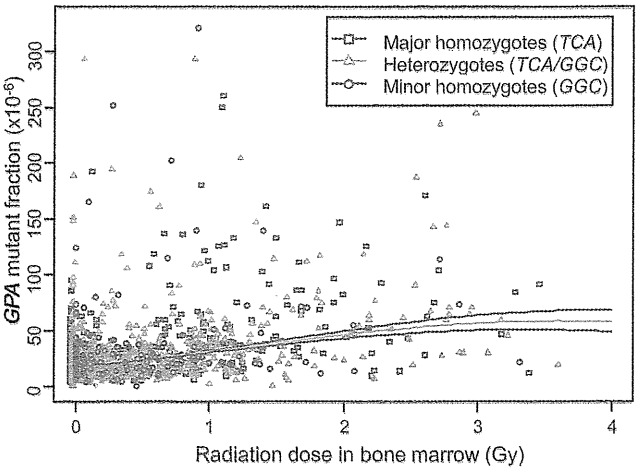

Fig. 1. *GPA* Mf dose response by *53BP1* haplotype. *GPA* Mf radiation-dose response (linear-quadratic) with a co-dominant genomic model for *53BP1* haplotype. Dose values are slightly offset to enhance visualization in dense regions. Each dot represents a single subject.

Next, we added cancer development as a further covariant in the regression analyses for *GPA* Mf, assuming that the dose response of *GPA* Mf would attenuate if the same DNA repair mechanism responsible for *GPA* mutation was also involved in somatic mutations leading to cancer. After adjustment for cancer, *GPA* Mf increased with radiation dose by a factor of 1.69 among *TCA* homozygotes and by 1.53 among *GGC* homozygotes (interaction $p = 0.024$)—the same values as obtained previously without adjustment for cancer.

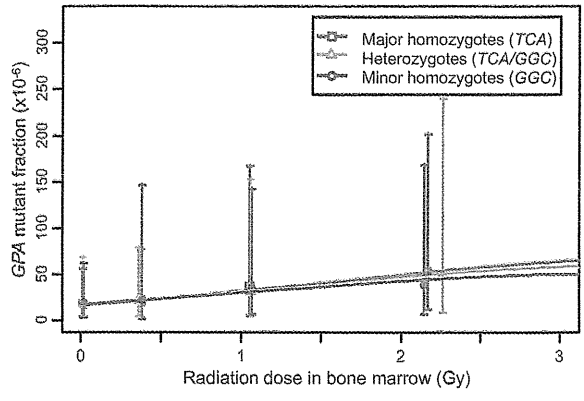

Fig. 2. *GPA* Mf dose response by *53BP1* haplotype (superimposed on grouped data). Plot from the same models as in Fig. 1 superimposed on grouped data. The error bars represent 95% confidence intervals.

4. Discussion

In this study, we found among atomic-bomb survivors a significant interaction between radiation dose and *53BP1* SNP-based genotype as well as the inferred haplotype in terms of *GPA* Mf. Although the *53BP1*-radiation interaction contributed slightly to overall variations in *GPA* Mf, the *53BP1* genotype contribution became more apparent with higher radiation doses. Thus, this study demonstrated for the first time that radiation-dose response of somatic mutations differed depending on DNA repair gene polymorphisms of individuals. Therefore, in the case of exposure to higher dose-radiation, persons having the *GGC* haplotype of *53BP1* may be more resistant to radiation-induced somatic mutation than those having the *TCA/TCA* haplotype. It is conceivable that *53BP1* genotype may be associated with DNA repair efficiency or accuracy, since this would make a bigger difference at higher doses, that is, when more DNA damage (likely to be repaired by 53BP1) occurs. In addition, we found no association of *53BP1* with cancer, which may be because the somatic mutation resulting from *53BP1*-mediated DNA repair is only one of many mechanisms involved in multi-stage carcinogenesis, and hence a causative factor in a part of radiation-associated cancers. Alternatively, it might turn out that the current study, with its population, has limited power to statistically detect genetic effects on cancer development.

Because observational data are often unable to detect interactions or infer the correct scale of joint effects, lack of statistical interaction for certain loci in the present analysis should not be construed as strong evidence either for or against biological interaction. A significant departure from additivity, however, can generally be considered as evidence of biological interaction [20]. Regarding genomic models, one-parameter models (linear, dominant, and recessive) were compared to assess what is the most appropriate scale for the genomic interaction (Table 6 and Supplementary Table 5). But choice of the correct genomic model, whether codominant or recessive, was not a certainty: deviances were 727.49 for the codominant model and 726.62 for the recessive model. Thus, looking at results from the statistical viewpoint, it is reasonable to conclude that there is evidence for a possible interaction between *53BP1* genotype and radiation on *GPA* Mf, but the nature of the interaction still needs to be clarified by other means, such as *in vitro* experiments, as discussed below.

Human erythrocytes have a limited cellular lifespan of around 120 days, and more than 60 years have passed since exposure to atomic-bomb radiation. So it may be that radiation-induced *GPA* mutations in atomic-bomb survivors have been recorded in longer-lived cell populations, most logically in HSC populations. Maintenance of genomic integrity is crucial for long-lived HSCs in order to prevent development of malignancies as well as loss of self-renewal and differentiation potentials [21,22]. Within the HSCs, various DNA damage including DSBs is assumed to be present as a result of physiological conditions or genotoxic insults. It has in fact been reported that DSBs accumulate in mouse and human HSC populations with aging, and the extent of accumulation of DNA damage appears to be dependent on DNA repair capacity [21–23]. Mouse-model studies in particular have demonstrated that DNA repair by the NHEJ pathway is a key determinant of HSC's ability to maintain genome integrity against genotoxic stress [21,22]. The present study of a human population is consistent with the mouse studies, indicating that DNA repair capacity by NHEJ plays a significant role in accumulation of somatic mutations in human HSCs.

Studies focused on molecular mechanisms of 53BP1 suggest that 53BP1 functions as a platform for other proteins in DNA-damage response: 53BP1 sensed DSBs after changes in higher-order chromatin structure, *i.e.*, binding to methylated histone residues that had been exposed in response to radiation exposure [24,25] and then recruited ATM to the break sites [8]. It is also known that

53BP1 increases chromatin mobility at DSB sites, thereby facilitating NHEJ repair in heterochromatin [26–28]. One nonsynonymous SNP (D353E) analyzed in this study is located in the N-terminal domains that have numerous irradiation-dependent phosphorylation sites by ATM and other kinases [29], another *53BP1* SNP (−885) is located in the putative regulatory region of the 5′ UTR [30]. Therefore, our findings may provide testable hypotheses that sequence variations in *53BP1* affect its function in DNA damage response: *e.g.*, radiation-induced focus formation involving 53BP1 at DSB sites, binding to methylated histones, or gene expression in irradiated HSCs. Such *in vitro* experiments could elucidate the underlying mechanisms of radiation-induced somatic mutagenesis associated with *53BP1* genetic variants, and add a fresh perspective to understanding the machinery for human HSC genome maintenance.

Conflict of interest

None declared.

Acknowledgements

The Radiation Effects Research Foundation (RERF), Hiroshima and Nagasaki, Japan is a private, non-profit foundation funded by the Japanese Ministry of Health, Labor and Welfare (MHLW) and the U.S. Department of Energy (DOE), the latter in part through DOE Award DE-HS0000031 to the National Academy of Sciences. This publication was supported by RERF Research Protocols RPs 3-87 and 4-04 and was supported in part by a Grant-in-Aid for Scientific Research (B) from the Ministry of Education, Culture, Sports, Science, and Technology of Japan (24390162), and a Grant-in-Aid for Cancer Research from the MHLW (22090501). The views of the authors do not necessarily reflect those of the two governments.

Appendix A. Supplementary data

Supplementary data associated with this article can be found, in the online version, at http://dx.doi.org/10.1016/j.mrgentox.2013.05.003.

References

[1] E. Pernot, J. Hall, S. Baatout, M.A. Benotmane, E. Blanchardon, S. Bouffler, H. El Saghire, M. Gomolka, A. Guertler, M. Harms-Ringdahl, P. Jeggo, M. Kreuzer, D. Laurier, C. Lindholm, R. Mkacher, R. Quintens, K. Rothkamm, L. Sabatier, S. Tapio, F. de Vathaire, E. Cardis, Ionizing radiation biomarkers for potential use in epidemiological studies, Mutat. Res. 751 (2012) 258–286.
[2] S. Kyoizumi, M. Akiyama, J.B. Cologne, K. Tanabe, N. Nakamura, A.A. Awa, Y. Hirai, Y. Kusunoki, S. Umeki, Somatic cell mutations at the glycophorin A locus in erythrocytes of atomic bomb survivors: implications for radiation carcinogenesis, Radiat. Res. 146 (1996) 43–52.
[3] S. Kyoizumi, Y. Kusunoki, T. Hayashi, M. Hakoda, J.B. Cologne, K. Nakachi, Individual variation of somatic gene mutability in relation to cancer susceptibility: prospective study on erythrocyte glycophorin a gene mutations of atomic bomb survivors, Cancer Res. 65 (2005) 5462–5469.
[4] N. Rothman, R. Haas, R.B. Hayes, G.L. Li, J. Wiemels, S. Campleman, P.J. Quintana, L.J. Xi, M. Dosemeci, N. Titenko-Holland, et al., Benzene induces gene-duplicating but not gene-inactivating mutations at the glycophorin A locus in exposed humans, Proc. Natl. Acad. Sci. U. S. A. 92 (1995) 4069–4073.
[5] C. Wyman, R. Kanaar, DNA double-strand break repair: all's well that ends well, Annu. Rev. Genet. 40 (2006) 363–383.
[6] B. Wang, S. Matsuoka, P.B. Carpenter, S.J. Elledge, 53BP1, a mediator of the DNA damage checkpoint, Science 298 (2002) 1435–1438.
[7] K. Nakamura, W. Sakai, T. Kawamoto, R.T. Bree, N.F. Lowndes, S. Takeda, Y. Taniguchi, Genetic dissection of vertebrate 53BP1: a major role in non-homologous end joining of DNA double strand breaks, DNA Repair (Amst.) 5 (2006) 741–749.
[8] T.A. Mochan, M. Venere, R.A. DiTullio Jr., T.D. Halazonetis, 53BP1, an activator of ATM in response to DNA damage, DNA Repair (Amst.) 3 (2004) 945–952.
[9] J.C. Morales, Z. Xia, T. Lu, M.B. Aldrich, B. Wang, C. Rosales, R.E. Kellems, W.N. Hittelman, S.J. Elledge, P.B. Carpenter, Role for the BRCA1 C-terminal repeats (BRCT) protein 53BP1 in maintaining genomic stability, J. Biol. Chem. 278 (2003) 14971–14977.
[10] R.A. DiTullio Jr., T.A. Mochan, M. Venere, J. Bartkova, M. Sehested, J. Bartek, T.D. Halazonetis, 53BP1 functions in an ATM-dependent checkpoint pathway that is constitutively activated in human cancer, Nat. Cell Biol. 4 (2002) 998–1002.
[11] I.M. Ward, K. Minn, J. van Deursen, J. Chen, p53 Binding protein 53BP1 is required for DNA damage responses and tumor suppression in mice, Mol. Cell. Biol. 23 (2003) 2556–2563.
[12] P.A. Jeggo, Risks from low dose/dose rate radiation: what an understanding of DNA damage response mechanisms can tell us, Health Phys. 97 (2009) 416–425.
[13] H. Ma, Z. Hu, X. Zhai, S. Wang, X. Wang, J. Qin, W. Chen, G. Jin, J. Liu, J. Gao, Q. Wei, H. Shen, Joint effects of single nucleotide polymorphisms in P53BP1 and p53 on breast cancer risk in a Chinese population, Carcinogenesis 27 (2006) 766–771.
[14] K. Chen, Z. Hu, L.E. Wang, W. Zhang, A.K. El-Naggar, E.M. Sturgis, Q. Wei, Polymorphic TP53BP1 and TP53 gene interactions associated with risk of squamous cell carcinoma of the head and neck, Clin. Cancer Res. 13 (2007) 4300–4305.
[15] C. He, H. Nan, A.A. Qureshi, J. Han, Genetic variants in the 53BP1 gene and skin cancer risk, J. Invest. Dermatol. 130 (2010) 2850–2853.
[16] K.J. Livak, Allelic discrimination using fluorogenic probes and the 5′ nuclease assay, Genet. Anal. 14 (1999) 143–149.
[17] S. Purcell, B. Neale, K. Todd-Brown, L. Thomas, M.A. Ferreira, D. Bender, J. Maller, P. Sklar, P.I. de Bakker, M.J. Daly, P.C. Sham, PLINK: a tool set for whole-genome association and population-based linkage analyses, Am. J. Hum. Genet. 81 (2007) 559–575.
[18] S. Greenland, W.D. Finkle, A critical look at methods for handling missing covariates in epidemiologic regression analyses, Am. J. Epidemiol. 142 (1995) 1255–1264.
[19] M.C. Cornelis, E.J. Tchetgen, L. Liang, L. Qi, N. Chatterjee, F.B. Hu, P. Kraft, Gene–environment interactions in genome-wide association studies: a comparative study of tests applied to empirical studies of type 2 diabetes, Am. J. Epidemiol. 175 (2012) 191–202.
[20] D. Thomas, Gene–environment-wide association studies: emerging approaches, Nat. Rev. Genet. 11 (2010) 259–272.
[21] A. Nijnik, L. Woodbine, C. Marchetti, S. Dawson, T. Lambe, C. Liu, N.P. Rodrigues, T.L. Crockford, E. Cabuy, A. Vindigni, T. Enver, J.I. Bell, P. Slijepcevic, C.C. Goodnow, P.A. Jeggo, R.J. Cornall, DNA repair is limiting for haematopoietic stem cells during ageing, Nature 447 (2007) 686–690.
[22] D.J. Rossi, D. Bryder, J. Seita, A. Nussenzweig, J. Hoeijmakers, I.L. Weissman, Deficiencies in DNA damage repair limit the function of haematopoietic stem cells with age, Nature 447 (2007) 725–729.
[23] C.E. Rube, A. Fricke, T.A. Widmann, T. Furst, H. Madry, M. Pfreundschuh, C. Rube, Accumulation of DNA damage in hematopoietic stem and progenitor cells during human aging, PLoS ONE 6 (2011) e17487.
[24] Y. Huyen, O. Zgheib, R.A. Ditullio Jr., V.G. Gorgoulis, P. Zacharatos, T.J. Petty, E.A. Sheston, H.S. Mellert, E.S. Stavridi, T.D. Halazonetis, Methylated lysine 79 of histone H3 targets 53BP1 to DNA double-strand breaks, Nature 432 (2004) 406–411.
[25] A. Xie, A. Hartlerode, M. Stucki, S. Odate, N. Puget, A. Kwok, G. Nagaraju, C. Yan, F.W. Alt, J. Chen, S.P. Jackson, R. Scully, Distinct roles of chromatin-associated proteins MDC1 and 53BP1 in mammalian double-strand break repair, Mol. Cell 28 (2007) 1045–1057.
[26] N. Dimitrova, Y.C. Chen, D.L. Spector, T. de Lange, 53BP1 promotes non-homologous end joining of telomeres by increasing chromatin mobility, Nature 456 (2008) 524–528.
[27] S. Difilippantonio, E. Gapud, N. Wong, C.Y. Huang, G. Mahowald, H.T. Chen, M.J. Kruhlak, E. Callen, F. Livak, M.C. Nussenzweig, B.P. Sleckman, A. Nussenzweig, 53BP1 facilitates long-range DNA end-joining during V(D)J recombination, Nature 456 (2008) 529–533.
[28] A.A. Goodarzi, A.T. Noon, D. Deckbar, Y. Ziv, Y. Shiloh, M. Lobrich, P.A. Jeggo, ATM signaling facilitates repair of DNA double-strand breaks associated with heterochromatin, Mol. Cell 31 (2008) 167–177.
[29] J.E. FitzGerald, M. Grenon, N.F. Lowndes, 53BP1: function and mechanisms of focal recruitment, Biochem. Soc. Trans. 37 (2009) 897–904.
[30] I. Dunham, A. Kundaje, S.F. Aldred, P.J. Collins, C.A. Davis, F. Doyle, C.B. Epstein, S. Frietze, J. Harrow, R. Kaul, J. Khatun, B.R. Lajoie, S.G. Landt, B.K. Lee, F. Pauli, K.R. Rosenbloom, P. Sabo, A. Safi, A. Sanyal, N. Shoresh, J.M. Simon, L. Song, N.D. Trinklein, R.C. Altshuler, E. Birney, J.B. Brown, C. Cheng, S. Djebali, X. Dong, J. Ernst, T.S. Furey, M. Gerstein, B. Giardine, M. Greven, R.C. Hardison, R.S. Harris, J. Herrero, M.M. Hoffman, S. Iyer, M. Kelllis, P. Kheradpour, T. Lassman, Q. Li, X. Lin, G.K. Marinov, A. Merkel, A. Mortazavi, S.C. Parker, T.E. Reddy, J. Rozowsky, F. Schlesinger, R.E. Thurman, J. Wang, L.D. Ward, T.W. Whitfield, S.P. Wilder, W. Wu, H.S. Xi, K.Y. Yip, J. Zhuang, B.E. Bernstein, E.D. Green, C. Gunter, M. Snyder, M.J. Pazin, R.F. Lowdon, L.A. Dillon, L.B. Adams, C.J. Kelly, J. Zhang, J.R. Wexler, P.J. Good, E.A. Feingold, G.E. Crawford, J. Dekker, L. Elinitski, P.J. Farnham, M.C. Giddings, T.R. Gingeras, R. Guigo, T.J. Hubbard, M. Kellis, W.J. Kent, J.D. Lieb, E.H. Margulies, R.M. Myers, J.A. Starnatoyannopoulos, S.A. Tennebaum, Z. Weng, K.P. White, B. Wold, Y. Yu, J. Wrobel, B.A. Risk, H.P. Gunawardena, H.C. Kuiper, C.W. Maier, L. Xie, X. Chen, T.S. Mikkelsen, S. Gillespie, A. Goren, O. Ram, X. Zhang, L. Wang, R. Issner, M.J. Coyne, T. Durham, M. Ku, T. Truong, M.L. Eaton, A. Dobin, T. Lassmann, A. Tanzer, J. Lagarde, W. Lin, C. Xue, B.A. Williams, C. Zaleski, M. Roder, F. Kokocinski, R.F. Abdelhamid, T. Alioto, I. Antoshechkin, M.T. Baer, P. Batut, I. Bell, K. Bell, S. Chakrabortty, J. Chrast, J. Curado, T. Derrien, J. Drenkow, E. Dumais, J. Dumais, R. Duttagupta, M. Fastuca, K. Fejes-Toth, P. Ferreira, S. Foissac, M.J. Fullwood, H. Gao, D. Gonzalez, A. Gordon, C. Howald, S. Jha, R. Johnson, P. Kapranov, B. King, C. Kingswood, G. Li, O.J. Luo, E. Park, J.B. Preall, K. Presaud, P. Ribeca, D. Robyr, X. Ruan, M. Sammeth, K.S. Sandu, L. Schaeffer, L.H. See, A. Shahab, J. Skancke, A.M. Suzuki, H. Takahashi, H. Tilgner, D. Trout, N.

Walters, H. Wang, Y. Hayashizaki, A. Reymond, S.E. Antonarakis, G.J. Hannon, Y. Ruan, P. Carninci, C.A. Sloan, K. Learned, V.S. Malladi, M.C. Wong, G.P. Barber, M.S. Cline, T.R. Dreszer, S.G. Heitner, D. Karolchik, V.M. Kirkup, L.R. Meyer, J.C. Long, M. Maddren, B.J. Raney, L.L. Grasfeder, P.G. Giresi, A. Battenhouse, N.C. Sheffield, K.A. Showers, D. London, A.A. Bhinge, C. Shestak, M.R. Schaner, S.K. Kim, Z.Z. Zhang, P.A. Mieczkowski, J.O. Mieczkowska, Z. Liu, R.M. McDaniell, Y. Ni, N.U. Rashid, M.J. Kim, S. Adar, Z. Zhang, T. Wang, D. Winter, D. Keefe, V.R. Iyer, K.S. Sandhu, M. Zheng, P. Wang, J. Gertz, J. Vielmetter, E.C. Partridge, K.E. Varley, C. Gasper, A. Bansal, S. Pepke, P. Jain, H. Amrhein, K.M. Bowling, M. Anaya, M.K. Cross, M.A. Muratet, K.M. Newberry, K. McCue, A.S. Nesmith, K.I. Fisher-Aylor, B. Pusey, G. DeSalvo, S.L. Parker, S. Balasubramanian, N.S. Davis, S.K. Meadows, T. Eggleston, J.S. Newberry, S.E. Levy, D.M. Absher, W.H. Wong, M.J. Blow, A. Visel, L.A. Pennachio, L. Elnitski, H.M. Petrykowska, A. Abyzov, B. Aken, D. Barrell, G. Barson, A. Berry, A. Bignell, V. Boychenko, G. Bussotti, C. Davidson, G. Despacio-Reyes, M. Diekhans, I. Ezkurdia, A. Frankish, J. Gilbert, J.M. Gonzalez, E. Griffiths, R. Harte, D.A. Hendrix, T. Hunt, I. Jungreis, M. Kay, E. Khurana, J. Leng, M.F. Lin, J. Loveland, Z. Lu, D. Manthravadi, M. Mariotti, J. Mudge, G. Mukherjee, C. Notredame, B. Pei, J.M. Rodriguez, G. Saunders, A. Sboner, S. Searle, C. Sisu, C. Snow, C. Steward, E. Tapanan, M.L. Tress, M.J. van Baren, S. Washieti, L. Wilming, A. Zadissa, Z. Zhengdong, M. Brent, D. Haussler, A. Valencia, A. Raymond, N. Addleman, R.P. Alexander, R.K. Auerbach, K. Bettinger, N. Bhardwaj, A.P. Boyle, A.R. Cao, P. Cayting, A. Charos, Y. Cheng, C. Eastman, G. Euskirchen, J.D. Fleming, F. Grubert, L. Habegger, M. Hariharan, A. Harmanci, S. Iyenger, V.X. Jin, K.J. Karczewski, M. Kasowski, P. Lacroute, H. Lam, N. Larnarre-Vincent, J. Lian, M. Lindahl-Allen, R. Min, B. Miotto, H. Monahan, Z. Moqtaderi, X.J. Mu, H. O'Geen, Z. Ouyang, D. Patacsil, D. Raha, L. Ramirez, B. Reed, M. Shi, T. Slifer, H. Witt, L. Wu, X. Xu, K.K. Yan, X. Yang, K. Struhl, S.M. Weissman, S.A. Tenebaum, L.O. Penalva, S. Karmakar, R.R. Bhanvadia, A. Choudhury, M. Domanus, L. Ma, J. Moran, A. Victorsen, T. Auer, L. Centarin, M. Eichenlaub, F. Gruhl, S. Heerman, B. Hoeckendorf, D. Inoue, T. Kellner, S. Kirchmaier, C. Mueller, R. Reinhardt, L. Schertel, S. Schneider, R. Sinn, B. Wittbrodt, J. Wittbrodt, G. Jain, G. Balasundaram, D.L. Bates, R. Byron, T.K. Canfield, M.J. Diegel, D. Dunn, A.K. Ebersol, T. Frum, K. Garg, E. Gist, R.S. Hansen, L. Boatman, E. Haugen, R. Humbert, A.K. Johnson, E.M. Johnson, T.M. Kutyavin, K. Lee, D. Lotakis, M.T. Maurano, S.J. Neph, F.V. Neri, E.D. Nguyen, H. Qu, A.P. Reynolds, V. Roach, E. Rynes, M.E. Sanchez, R.S. Sandstrom, A.O. Shafer, A.B. Stergachis, S. Thomas, B. Vernot, J. Vierstra, S. Vong, M.A. Weaver, Y. Yan, M. Zhang, J.A. Akey, M. Bender, M.O. Dorschner, M. Groudine, M.J. MacCoss, P. Navas, G. Stamatoyannopoulos, J.A. Stamatoyannopoulos, K. Beal, A. Brazma, P. Flicek, N. Johnson, M. Lukk, N.M. Luscombe, D. Sobral, J.M. Vaquerizas, S. Batzoglou, A. Sidow, N. Hussami, S. Kyriazopoulou-Panagiotopoulou, M.W. Libbrecht, M.A. Schaub, W. Miller, P.J. Bickel, B. Banfai, N.P. Boley, H. Huang, J.J. Li, W.S. Noble, J.A. Bilmes, O.J. Buske, A.O. Sahu, P.V. Kharchenko, P.J. Park, D. Baker, J. Taylor, L. Lochovsky, An integrated encyclopedia of DNA elements in the human genome, Nature 489 (2012) 57–74.

Age-Associated Changes in the Differentiation Potentials of Human Circulating Hematopoietic Progenitors to T- or NK-Lineage Cells

Seishi Kyoizumi,* Yoshiko Kubo,* Junko Kajimura,* Kengo Yoshida,* Kazue Imai,* Tomonori Hayashi,* Kei Nakachi,* Lauren F. Young,† Malcolm A. Moore,‡ Marcel R. M. van den Brink,† and Yoichiro Kusunoki*

Age-associated changes of T and NK cell (T/NK) potential of human hematopoietic stem cells are unknown. In this study, we enumerate and characterize T/NK precursors among $CD34^+Lin^-$ cell populations circulating in normal human adult peripheral blood (PB) by a limiting-dilution assay using coculture with OP9-DL1 stroma cells expressing Notch 1 ligand, Delta-like 1. The frequency of T cell precursors in $CD34^+Lin^-$ cells was found to decrease with donor age, whereas the ratio of NK to T cell precursor frequency (NK/T ratio) increased with age, suggesting that lymphoid differentiation potential of PB progenitors shifts from T to NK cell lineage with aging. Clonal analyses of $CD34^+Lin^-$ cells showed that differences in the NK/T ratio were attributable to different distributions of single- and dual-lineage T/NK precursor clones. Because nearly all of the clones retained monocyte and/or granulocyte differentiation potentials in coculture with OP9-DL1 cells, T/NK precursors in PB are considered to be contained in the pool of T/NK/myeloid multipotent progenitors. The age-associated increase in NK over T cell commitment might occur in precursor cells with T/NK/myeloid potential. *The Journal of Immunology*, **2013, 190: 6164–6172.**

One of the most characteristic features of immunological aging is the decline of T cell production associated with thymic involution. Consequently, the peripheral naive T cell pool gradually reduces in size during aging. The main causes of age-associated thymic dysfunction are thought to involve impairments in both hematopoietic stem cells (HSCs) and thymic microenvironment (1–3). Studies in mice have shown the age-related loss of T cell potential in both prethymic and intrathymic progenitors (4, 5), and a recent report suggested that human HSCs exhibited myeloid-biased differentiation potentials with aging (6). Furthermore, a recent paper reported that T cell potential was lower in human adult bone marrow (BM) than cord blood (CB), suggesting high T cell potential in human neonate HSCs (7). However, precise age-associated changes in the T cell potential of human adult HSCs and downstream progenitors have not been well characterized.

In contrast with age-associated decline in T cell development, both the proportion and absolute number of NK cells in the periphery have been reported to increase with age (8–10). These findings suggest that aging has either no effect or a positive effect on NK-lineage differentiation, which could lead to the observed increase in peripheral NK cells. The T/NK-lineage differentiation pathway is well defined, and it is widely accepted that both T and NK cells are generated from bipotent T/NK progenitors (11). We hypothesize that the bifurcation of T/NK coprogenitors shifts from T to NK cell lineage with aging, leading to the differences observed in T and NK cell numbers and proportions with aging. In addition to this, we hypothesize that the microenvironment supporting NK production may be unchanged or enhanced during aging in stark contrast to the decline of microenvironment for T cell development.

To test the above hypotheses, we sought to establish in vitro functional and quantitative analyses of T and NK cell progenitors using peripheral blood (PB). Human PB was used as a source of progenitor cells because of the low availability of human tissue specimens and also because T/NK cell precursors are assumed to migrate from BM to the thymus through the bloodstream (12, 13). However, the entity of thymic immigrants for T/NK cell differentiation is rather controversial, although extensive studies have been conducted in mouse thymus, PB, and BM. Contrary to the classical model of hematopoiesis positing the earliest segregation of lymphoid and myeloid lineages, recent studies revealed that thymic immigrants possessed myeloid potential in addition to harboring T/NK cell potentials in mice (14–16). These results are concordant with previous findings that the only progenitors in blood with efficient T-lineage potential are multipotent progenitors (MPPs) with Lin^-Sca1^+ and $c\text{-}Kit^+$ phenotypes including lymphoid-primed MPPs (LMPPs) and that no common lymphoid progenitors (CLPs) were detected in mouse blood (17). Con-

*Department of Radiobiology/Molecular Epidemiology, Radiation Effects Research Foundation, Hiroshima 732-0815, Japan; †Department of Medicine and Immunology, Memorial Sloan-Kettering Cancer Center, New York, NY 10065; and ‡Cell Biology Program, Memorial Sloan-Kettering Cancer Center, New York, NY 10065

Received for publication November 20, 2012. Accepted for publication April 6, 2013.

This work was supported by the Radiation Effects Research Foundation (Hiroshima and Nagasaki, Japan), a private, nonprofit foundation funded by the Japanese Ministry of Health, Labor, and Welfare and the U.S. Department of Energy, the latter in part through Department of Energy Award DE-HS0000031 to the National Academy of Sciences. This study was based on Radiation Effects Research Foundation Research Protocol RP 5-09 and was supported by the U.S. National Institute of Allergy and Infectious Diseases (Contract HHSN272200900059C).

The views of the authors do not necessarily reflect those of the two governments.

Address correspondence and reprint requests to Dr. Seishi Kyoizumi and Dr. Yoichiro Kusunoki, Department of Radiobiology/Molecular Epidemiology, Radiation Effects Research Foundation, 5-2 Hijiyama Park, Minami Ward, Hiroshima 732-0815, Japan. E-mail addresses: kyoizumi@rerf.or.jp (S.K.) and ykusunok@rerf.or.jp (Y.K.)

The online version of this article contains supplemental material.

Abbreviations used in this article: BM, bone marrow; BMMC, bone marrow mononuclear cell; CB, cord blood; CLP, common lymphoid progenitor; cytCD3, cytoplasmic CD3ε; FL, Flt-3 ligand; HSC, hematopoietic stem cell; KL, Kit ligand; LDA, limiting-dilution assay; LMPP, lymphoid-primed multipotent progenitor; MPP, multipotent progenitor; PB, peripheral blood; WB, washing buffer.

www.jimmunol.org/cgi/doi/10.4049/jimmunol.1203189

trasting reports have described a small number of CLPs in mouse blood that can produce T cell–lineage progeny in vitro and in the thymus (18–20). A more recent report revealed that lymphoid-restricted progenitors were the major route to T cell lineage in vivo despite their myeloid potential in vitro and that myeloid cells in the thymus originated from different precursors than T cells did under physiological conditions (21). Thus, as suggested in the previous studies, thymic progenitors in mice are thought to be multiple progenitor populations including CLPs and upstream LMPPs (12, 22). In humans, although recent work with BM and CB progenitors demonstrated the existence of analogous lymphoid progenitors with myeloid potential (23), lymphoid precursors circulating in adult PB have not been identified.

In this study, we describe a cell sorting–based limiting-dilution assay (LDA) and clonal analyses for quantifying and characterizing T/NK progenitors among $CD34^+Lin^-$ cell populations in the PB of healthy adult humans. We did not use any lymphoid progenitor-specific markers to isolate progenitors, because some mouse studies suggested that CLPs as well as more upstream progenitors with lymphoid potential can circulate in the blood, as mentioned above (17, 22). Because the $CD34^+Lin^-$ cell population is believed to contain all classes of hematopoietic progenitors including myeloid progenitors, CLPs, LMPPs, MPPs, and HSCs (13, 23), we used selective culture conditions to analyze T/NK lineage. T cell differentiation can be induced in human CB $CD34^+$ cells by coculture with OP9-DL1 stroma cells expressing the Notch 1 ligand Delta–like 1 and IL-7 and Flt-3 ligand (FL) (24). Activation of Notch 1 signaling also contributes to the efficient development of NK cells in humans (25, 26). It has recently been reported that Notch signaling in combination with IL-7, FL, and Kit ligand (KL), can induce NK-lineage differentiation in CB $CD34^+$ cells in the absence of IL-15 (27). Thus, both T and NK cell differentiation can simultaneously be analyzed by the combination of OP9-DL1 coculture with those three cytokines.

Using the assays, we examined age-associated changes of PB T/NK precursor frequencies in healthy adult humans. We found that the T cell precursor frequency significantly decreased with age, whereas NK cell precursor frequency did not. The findings suggest an age-associated shift of lymphoid differentiation potential from T to NK cell lineage in PB progenitors.

Materials and Methods

Cytokines and Abs

Recombinant human KL, FL, IL-3, IL-7, and IL-15 were purchased from PeproTech. Erythropoietin was purchased from Invitrogen. Anti-CD3 (SK7), cytoplasmic CD3ε (cytCD3; UCHT1), CD4 (SK-3), CD5 (UCHT2), CD7 (M-T701), CD8 (SK1), CD16 (3G8), CD19 (HIB19), CD20 (2H7), glycophorin A (GA-R2), and IFN-γ (25723.11) Abs were purchased from BD Biosciences. Anti-CD16a (3G8), CD34 (581), CD56 (N901), and CD159a (Z199) Abs were purchased from Beckman Coulter. Anti-CD14 (TÜK4) and granzyme B (GB12) Abs were purchased from Invitrogen. Anti-CD161 (HP-3G1) Ab was purchased from eBioscience.

Cell preparation

Human PB samples were collected from 16 healthy in-house volunteer donors (Japanese) with informed consent, following the guidance of the institutional review board (Human Investigation Committee of Radiation Effects Research Foundation), which approved this study. PBMCs were separated from 10-ml PB samples by Ficoll density gradient centrifugation (Lymphocyte Separation Medium 1077; Wako Pure Chemical Industry). Normal BM mononuclear cells (BMMCs) (Caucasian) were purchased from Lonza Walkersville.

Stroma cells

Generation of the mouse OP9-DL1 stroma cells engineered to express the GFP and the mouse *Delta-like 1* gene has been described previously (28). The OP9-DL1 and the OP9 (29) parental stroma cells were maintained by culturing in α-MEM (Life Technologies) supplemented with 20% FBS (Hyclone), 4×10^{-6} M 2-ME, and penicillin–streptomycin at 37°C in a humidified atmosphere flushed with 5% CO_2.

LDA of T/NK precursors

For progenitor cell culture, OP9-DL1 stroma cells were seeded in wells (50–80% confluence) precoated with 0.1% gelatin (Millipore) of a 384-well flat-bottom black plate (BD Biosciences). At least 4 h prior to progenitor cell sorting, culture medium in each well was replaced by 50 μl phenol red-free α-MEM containing 20% knockout serum replacement (Life Technologies), 10^{-4} M monothioglycerol (Sigma-Aldrich), 50 μg/ml gentamicin (Sigma-Aldrich), 10 ng/ml KL, 10 ng/ml FL, and 10 ng/ml IL-7 (T/NK medium). For progenitor cell sorting, PBMCs and BMMCs were stained with allophycocyanin-conjugated anti-CD34 Ab and PE-conjugated anti-lineage markers (anti-CD3, CD14, CD16, CD19, CD20, CD56, and glycophorin A Abs) for 30 min on ice, and dead cells were excluded by 1 μg/ml propidium iodide staining (BD Bioscience), as shown in Fig. 1A. One thousand $CD34^+Lin^-$ cells were sorted into 80 wells of a 384-well plate at the frequency of 20, 15, 10, or 5 cells/well (20 wells for each cell frequency) by FACSAria II (BD Biosciences). Surrounding wells were filled with PBS containing antibiotics for reducing evaporation of culture medium. LDA culture was maintained at 37°C in a humidified atmosphere flushed with 5% CO_2. One-half of culture medium (25 μl) was changed every week.

After 5 wk of culture, all cells grown in wells were harvested by vigorous pipetting and washed with PBS containing 2 mM EDTA, 0.01% NaN_3, and 1% FBS (washing buffer [WB]). For detection of T- and NK-lineage progenies by Cyan (Beckman Coulter), cells were stained with allophycocyanin-conjugated CD5, PE-conjugated CD7, and PE–Cy7-conjugated CD56 Abs in WB. Stained cells were resuspended with 200 μl WB containing 1 μg/ml DAPI (Invitrogen) to exclude dead cells by flow cytometry. OP9-DL1 cells and their cell debris were gated out using GFP fluorescence. $CD7^+CD5^+$ and $CD7^+CD56^+$ cells appeared in the constantly gated-fluorescence region were defined as T- and NK-lineage progenies, respectively. Absolute numbers of each progeny per well were calculated from the number of events on a flow cytogram in a volume (160 μl) of cell suspension. A well exhibiting six positive events and over was designated as a positive well. Frequencies of T and NK cell precursors were calculated by online analysis using ELDA software (30), available on the homepage of Walter Elisa Hall Institute Bioinformatics Division (http://bioinf.wehi.edu.au/software/elda/index.html). This software is based on a single-hit model and has a test of adequacy of the single-hit hypothesis and tests for frequency differences between multiple data sets.

For differentiation kinetics and phenotype analyses, $CD34^+Lin^-$ cells were cultured in some experiments at 500 cells/well using a 24-well plate in the same conditions as those used for the 384-well plates.

Clonal analysis

$CD34^+Lin^-$ cells from each donor were sorted (one cell per well) into a total of more than 560 wells using 384-well plates at a single cell per well. The culture conditions were the same as those for LDA, as described above. All cells in a well of a 384-well plate exhibiting generation of progenies after 5-wk culture were transferred to a well of a 96-well plate, where OP9-DL1 cells were preseeded. After culture for 5–10 d in the presence of KL, IL-7, and FL, cells were analyzed for T/NK-lineage markers, as described above.

Phenotyping of T/NK progenies

To determine the stage of T cell maturation, progeny cells were stained with PerCP-conjugated CD3, Pacific Blue–conjugated CD4, and allophycocyanin–Cy7-conjugated CD8 Abs in combination with CD5, CD7, and CD56 Abs. For characterization of NK-lineage progenies, cells were stained with PE-conjugated CD159a and PerCP–Cy5.5-conjugated CD161 Abs in combination with CD5, CD7, and CD56 Abs. Cytoplasmic expressions of granzyme B, CD3ε, and IFN-γ in NK-lineage progenies were analyzed by sorting cultured $CD7^+CD56^+$ cells. The cells were fixed and permeabilized using FACS permeabilizing solution (BD Biosciences) and stained with PE-conjugated anti-granzyme B, FITC-conjugated anti-CD3, or FITC-conjugated anti–IFN-γ Abs. Further maturation of $CD7^+CD56^+$ cells was induced by culture in T/NK-medium containing IL-15 (10 ng/ml) in the absence of stroma cells for 2–3 wk. Surface expressions of CD159a and CD161 and cytoplasmic expressions of granzyme B, CD3, and IFN-γ in the IL-15–induced cells were analyzed by the same procedures as described above.

Phenotyping of myeloid progenies

The presence of myeloid progenies in clonal cultures was determined by staining with PE-conjugated CD14 and PerCP-conjugated CD16 Abs for

monocytes and granulocytes, respectively, in combination with CD5, CD7, and CD56 Abs. For morphological identification of myeloid lineage, clonal cells in wells exhibiting $CD7^+CD5^+$ and/or $CD7^+CD56^+$ progenies were pooled and stained with PE-conjugated CD7, allophycocyanin Alexa Fluor 750-conjugated CD14, and PerCP-Cy5.5 CD16 Abs. Either $CD7^-CD14^+CD16^-$ (monocytes) or $CD7^-CD14^+CD16^+$ (granulocytes) cells were sorted into a droplet (25 μl PBS containing 2% BSA) on a glass slide and stained with May–Giemsa.

Methylcellulose colony assay

CFU-GM and burst-forming unit erythroid were assayed by methylcellulose cultures, according to previously described methods (31). Briefly, PBMCs were plated in 24-well plates at a concentration of 2.5×10^5/ml in 0.25-ml culture containing 1.2% methylcellulose (Stem Cell Technology) with erythropoietin (6 U/ml), KL (20 ng/ml), G-CSF (20 ng/ml), and IL-3 (20 ng/ml). The methylcellulose cultures were counted after 14 d to determine the number of colonies per well.

Statistics

Spearman's rank correlation analysis and Mann–Whitney U and χ^2 tests were conducted using SPSS 16.01 software (SPSS).

Results

LDA of T/NK precursors in $CD34^+Lin^-$ cells

PB and BM $CD34^+Lin^-$ cells (Fig. 1A) were cultured with OP9-DL1 stroma cells in the presence of KL, FL, and IL-7. Generation of T- and NK-lineage progeny in OP9-DL1 cultures was determined by flow cytometric detection of $CD7^+CD5^+$ and $CD7^+CD56^+$ progenies, respectively (Fig. 1B). Although variation among individual donors was large, the absolute numbers of both progenies per well on average were found to reach plateau levels after 5 wk of culture in both 24- and 384-well plates (Fig. 1 C–E). When we seeded 20 $CD34^+Lin^-$ cells into wells of 384-well plates, we observed in approximately half of the wells the development of $CD7^+CD5^+$ or $CD7^+CD56^+$ cells, but the numbers of T/NK progenies could differ 100-fold from well to well (Fig. 1E). On the basis of the distribution of positive events in coculture of $CD34^+Lin^-$ cells with OP9 control cells (Fig. 2A), we determined six positive events and over per well as the cutoff value for a positive well in LDA. Using this cutoff value, we confirmed that

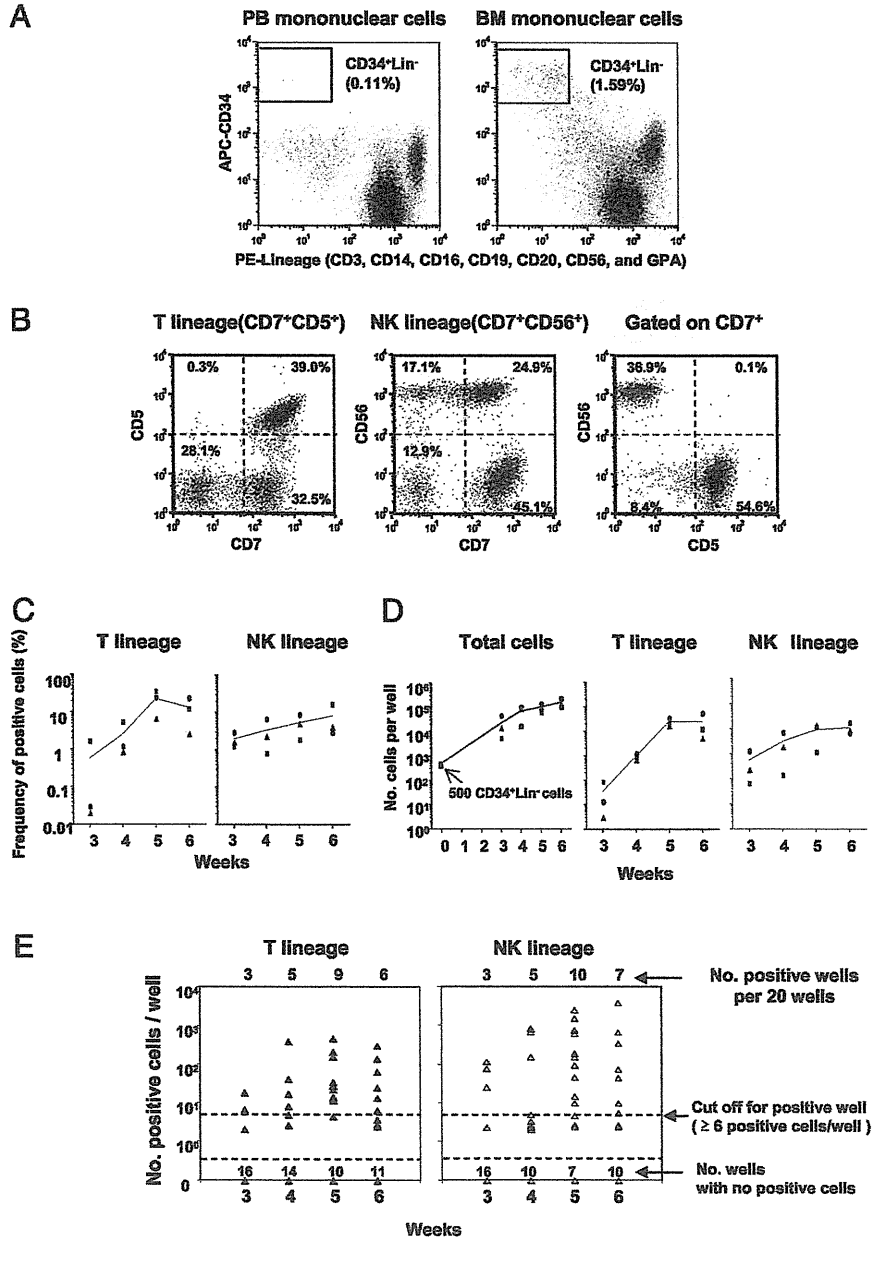

FIGURE 1. Growth and differentiation kinetics of T/NK-lineage progenies generated from PB $CD34^+Lin^-$ cells. (**A**) Representative flow cytograms of $CD34^+Lin^-$ cells in PB (*left panel*) and BM (*right panel*) mononuclear cells. (**B**) Representative flow cytograms of $CD5^+$ $CD7^+$ T-lineage (*left panel*) and $CD7^+CD56^+$ NK-lineage (*middle panel*) progenies generated from PB $CD34^+Lin^-$ cells in 5-wk OP9-DL1 coculture in the presence of KL, IL-7, and FL. CD5 and CD56 were expressed in different cell populations of $CD7^+$ cells (*right panel*). (**C** and **D**) Time courses of T- and NK-lineage differentiation of PB $CD34^+Lin^-$ cells. PB $CD34^+$ Lin^- cells from three donors were cultured at the concentration of 500 cells/well in a 24-well plate, where OP9-DL1 stroma cells were preseeded in the presence of KL, IL-7, and FL. Percentage (C) and absolute number (D) of $CD7^+CD5^+$ T- and $CD7^+CD56^+$ NK-lineage progenies generated from $CD34^+Lin^-$ cells are plotted against time (weeks). Solid lines connect the average values. (**E**) Time course of T- and NK-lineage differentiation from $CD34^+$ Lin^- cells from one donor. Each dot represents the total number of $CD7^+CD5^+$ (*left panel*) or $CD7^+CD56^+$ (*right panel*) cells generated from 20 $CD34^+Lin^-$ cells in a well of 384-well plate. Twenty wells were analyzed for each of 3, 4, 5, and 6 wk. A well exhibiting six and greater positive events was determined to be a positive well for LDA. Similar results were obtained from two experiments for the other two donors.